

Electrically Responsive Materials and Devices Directly Driven by the High Voltage of Triboelectric Nanogenerators

Jinhui Nie, Xiangyu Chen,* and Zhong Lin Wang*

Smart materials with electrically responsive characteristics and devices relying on different electrostatic effects can be directly driven by triboelectric nanogenerators (TENGs). The open circuit voltage from a TENG can easily reach thousands of volts with a separation distance of a few millimeters and this high output voltage can be used to effectively drive or control some devices with high internal resistance. This kind of combination is the most straightforward way for achieving a self-powered smart system. Hence, a detailed survey of electrically responsive materials and devices that can be successfully combined with TENG is summarized, including dielectric elastomers, piezoelectric materials, ferroelectric materials, electrostatic manipulators, electrostatic air cleaners, and field emission and mass spectrometers. Moreover, key factors in determining suitable materials or devices to work with TENG are clarified and an in-depth discussion of the current challenges related to these combined systems is provided. With the cost-effectiveness and simple manufacturing process, these TENG-based composite systems have great application prospects in the field of smart mechanics, human-machine interaction systems, intelligent storage systems, self-powered microfluidic chips, portable mass spectrometers, and so on.

1. Introduction

Invented in 2012, a fundamental energy technology, triboelectric nanogenerator (TENG), has been quickly developed to be a

mainstream technique in the field of energy harvesting and self-powered systems.^[1] Based on the coupling effect of triboelectrification and electrostatic induction,^[2] TENG can convert almost all kinds of mechanical energies from vibrations, water waves, wind, raindrop, and human motions into electricity.^[3] Comparing with other energy harvesting techniques, TENG is more attractive because of its advantages of simple fabrication, reliability, cost-effectiveness, and wide availability of low-frequency resources.^[4] The TENG can serve as a sustainable power supply^[5] by developing four different operation modes,^[6] including vertical contact-separation mode,^[7] lateral sliding mode,^[8] single-electrode mode,^[9] and freestanding triboelectric-layer mode.^[10] Meanwhile, in order to improve the output performance of TENG, a great number of works have been done to optimize the materials and interfaces of the device.^[11] Accordingly, the optimized TENG performance can achieve

an area power density larger than 500 W m^{-2} ,^[12] a volume power density about 15 MW m^{-3} ,^[12] an instantaneous conversion efficiency larger than 70%,^[13] and a total efficiency up to 85%.^[14] As an advanced and durable energy source, the development of TENG has promoted and inspired many fields, such as wind^[15] and ocean energy harvesting,^[16] self-powered smart systems,^[17] potable energy package,^[18] highly sensitive tactile sensor,^[19] and so on.

Generally speaking, the output characteristic of TENG is a high open-circuit voltage (V_{OC}) reaching a few thousand volts and a low short-circuit current (I_{sc}) at the scale of microampere.^[20] The output voltage from TENG decreases dramatically with the decrease of the load resistance. Thus, TENG is good for directly controlling some capacitive devices with a rather high internal resistance.^[21] Considering this output performance, many electrically responsive materials and devices, including dielectric elastomer, ferroelectric polymer, field emission devices, and so on, can be directly driven by TENG, which brings out a series of self-powered smart systems with various intriguing functions. By selecting the detailed operating parameters, output voltage and transferred charges of TENG can be precisely controlled, which can be parameterized for driving and manipulating these systems. Meanwhile, TENG can serve as a bridge for human-machine interactions, since it instantaneously converts human motions into electrical signals. Accordingly, both static and dynamic

J. Nie, Prof. X. Chen, Prof. Z. L. Wang
Beijing Key Laboratory of Micro-Nano Energy and Sensor
Beijing Institute of Nanoenergy and Nanosystems
Chinese Academy of Sciences
Beijing 100083, P. R. China
E-mail: chenxiangyu@binn.cas.cn; zlwang@gatech.edu

J. Nie, Prof. X. Chen, Prof. Z. L. Wang
School of Nanoscience and Technology
University of Chinese Academy of Sciences
Beijing 100049, P. R. China

Prof. X. Chen, Prof. Z. L. Wang
Center on Nanoenergy Research
School of Physical Science and Technology
Guangxi University
Nanning, Guangxi 530004, P. R. China

Prof. Z. L. Wang
School of Material Science and Engineering
Georgia Institute of Technology
Atlanta, GA 30332-0245, USA

 The ORCID identification number(s) for the author(s) of this article can be found under <https://doi.org/10.1002/adfm.201806351>.

DOI: 10.1002/adfm.201806351

mechanical excitation can be used as a trigger or control signal for many electromechanical systems. Moreover, the limited tribo-charges induced by TENG are consumed rapidly when the electrical breakdown is about to happen, which can be considered as a kind of very sensitive self-protection mechanism to reduce the risk of electrical damage for many high-voltage devices. These characteristics determine that TENG can serve as an efficient high-voltage source with excellent controllability and reliable safety for many smart systems and devices.

Both the smart materials with different electrically responsive characteristics and the different electrostatic devices can be possibly coupled with TENG to establish a composite system with various practical functions, which leads to a simple but effective way to achieve a self-powered smart system. In this review, we focus on the latest developments of the self-powered systems based on this kind of combinations, and we also provide a clear understanding of the key factors for determining whether the chosen materials or devices can be successfully combined with TENG. **Figure 1** shows the theme of this article and several typical examples for utilizing the high voltage of TENG. In the first segment of the review, we give an in-depth introduction of the successful approaches taken for achieving a high voltage of TENG. In the subsequent sections, we give a detailed overview of the electrically responsive materials and electrostatic devices that can be effectively driven by the TENG, including dielectric elastomers, piezoelectric materials, ferroelectric materials, electrostatic manipulator, electrostatic air cleaner, field emission, and mass spectrometer. Finally, a broader perspective and the proposing future research directions are discussed to conclude the review.

2. Overview of Materials and Methods for TENG

In order to effectively drive and control various TENG-based functional systems, the output voltage of TENG needs to be maintained at a high level. The operating principle of TENG is based on the integrated effect of triboelectrification and electrostatic induction. Hence, there are two approaches to maximize the output voltage of TENG. One is to reduce the parasitic capacitance at the maximum separated distance of TENG.^[28] In order to maximize the open-circuit voltage and the amount of transferred charge, the capacitance variation of TENG should be maximized. To study the specific situation in the actual operation, researchers have designed four different operation modes for TENG and established a structure analyzing method based on finite element simulation, which can calculate optimized structure parameters for TENG.^[29] Another approach is to enhance the surface charge density generated on the surface of tribo materials. By increasing the amount of triboelectric charge and contact charge, the induced charge is increased, and then the output performance of TENG can be fundamentally improved. The related surface modification methods can be universally applied to TENG with various structures. Therefore, maximizing surface charge density is the basic strategy for realizing high output voltage of TENG. This section will discuss the most commonly used methods for increasing surface charge density.



Jinhui Nie received his bachelor's degree in Applied Chemistry at Shandong University in 2015. Now he is a doctoral candidate in Beijing Institute of Nanoenergy and Nanosystem, Chinese Academy of Sciences. His current research mainly focuses on triboelectric nano-generators and their applica-

tions in the self-powered microfluidic transport system and energy storage.



Xiangyu Chen received his B.S. degree in Electrical Engineering from Tsinghua University in 2007 and his Ph.D. in Electronics Physics from Tokyo Institute of Technology in 2013. Now he is a professor in Beijing Institute of Nanoenergy and Nanosystems, Chinese Academy of Sciences. His main research interests have

been focused on the field of functional dielectric materials, self-powered nanoenergy system and the nonlinear optical laser system for characterizing the electrical properties of the devices.



Zhong Lin (Z. L.) Wang is the Hightower Chair in Materials Science and Engineering and Regents' Professor at Georgia Tech, the Chief Scientist and Director of the Beijing Institute of Nanoenergy and Nanosystems, Chinese Academy of Sciences. His discovery and breakthroughs in developing nanogenerators and self-powered nanosys-

tems establish the principle and technological roadmap for harvesting mechanical energy from environmental and biological systems for powering personal electronics and future sensor networks. He coined and pioneered the field of piezotronics and piezophotonics.

2.1. Materials Selection

Almost all materials have triboelectrification effects, including metals, polymers, wood, and so on; thus, the number of candidate materials for TENG is huge. The detailed physical mechanism of the contact electrification effect happened with

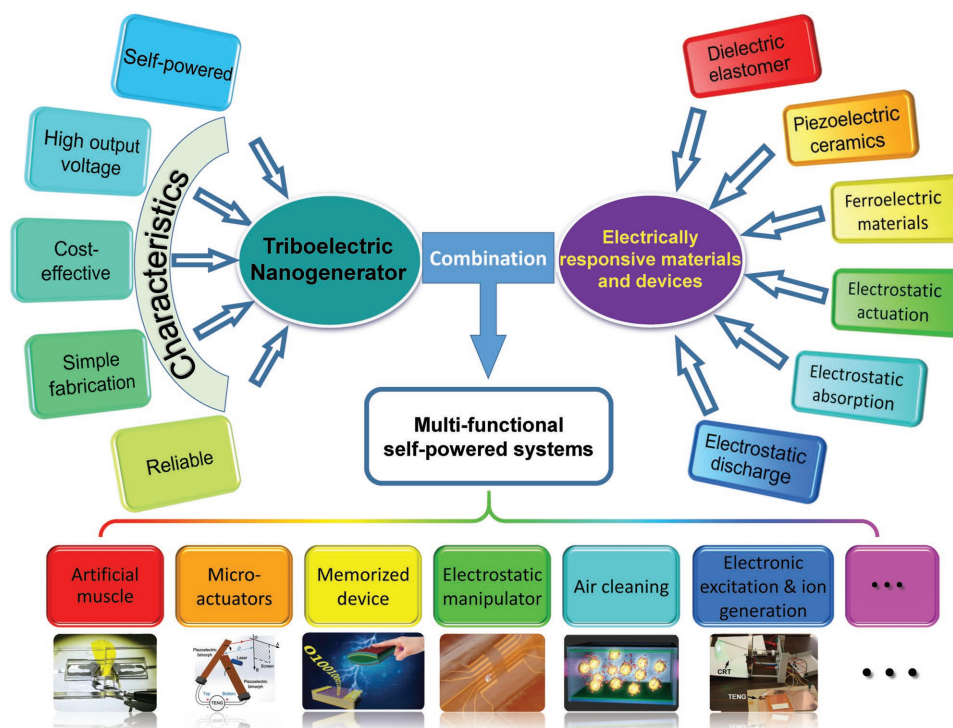


Figure 1. Combination of TENG and electrically responsive materials/devices for functional self-powered systems. Artificial muscle: adapted with permission.^[22] Copyright 2016, Wiley-VCH. Micro-actuators: adapted with permission.^[23] Copyright 2014, Wiley-VCH. Memorized device: adapted with permission.^[24] Copyright 2015, Royal Society of Chemistry. Electrostatic manipulator: adapted with permission.^[25] Copyright 2018, American Chemical Society. Air cleaning: adapted with permission.^[26] Copyright 2015, American Chemical Society. Electronic excitation & ion generation: adapted with permission.^[27] Copyright 2018, Wiley-VCH.

different materials is still under investigation and many theories and considerations have been continuously developed for many years.^[30] Generally speaking, the triboelectric charge density is highly dependent on the electron affinity difference between the two contact materials. Therefore, the choice of two materials with a large difference in electron affinity to prepare TENG can increase the induced triboelectric charges. Some common materials with different electron affinity are listed in Table S1 in the Supporting Information, which was published by Henniker^[31] in 1962, by Davies^[32] in 1969, and by Lee^[33] in 2009. Although there are some differences among the sequences tested by different researchers, these series can provide good guidance for materials selection in TENG design. For example, the friction between the material from the bottom and the top of the list will result in a large charge density. On the other hand, the summarized materials list in Table S1 in the Supporting Information can also help to design some special TENG for different application purposes. For example, silicone rubber with good stretchability and durability can be used to fabricate flexible and wearable energy harvester;^[34] the Teflon or Kapton tape with a smooth surface and abrasive resistance can be considered as the tribo material for long-life sliding TENG.^[35] Meanwhile, the polyethylene terephthalate (PET) or fluorinated ethylene propylene (FEP) film with good transparency can be applied to the TENG-based smart device.^[36] Therefore, materials selection is the first step for fabrication of TENG. The electron affinity list can help us to determine the candidate materials for TENG devices.

2.2. Surface Modification of Materials

To enhance the output voltage of TENG, surface modification is also a very effective method for boosting the tribo-charge density. The frictional area can be increased by microscopically changing the physical structure of the tribo-material surface, and then the amount of tribo-induced charge is increased upon contact friction. **Figure 2** contains several representative examples of surface modifications and their output performance comparisons. Figure 2a shows the scanning electron microscope (SEM) images of three different surface types: line, cube, and pyramid, with insets showing the corresponding enlarged cross-sectional views of the linear, cubic, and pyramidal structures.^[37] These micropatterns are produced from the relative silicon moulds. Figure 2b compares the output voltage of a typical contact-separation TENG with four different surface types: plane (unstructured), line, cube, and pyramid. The measured V_{OC} of the TENGs with four different feature types clearly followed an order of plane < line < cube < pyramid. In addition, V_{OC} of the pyramid-featured device is almost four times as high as that of the plane one. Lee et al. also prepared the roughness of the polydimethylsiloxane (PDMS) surface by using micro-nanostructured Al as a nanoimprinting template.^[38] The performance of the related TENG can be further improved by introducing nanostructure on the tribo-surface with microroughness, which proves that the scale of surface roughness can also influence the performance of TENG. Selective dry etching and inductively coupled plasma (ICP) etching^[39] as simple

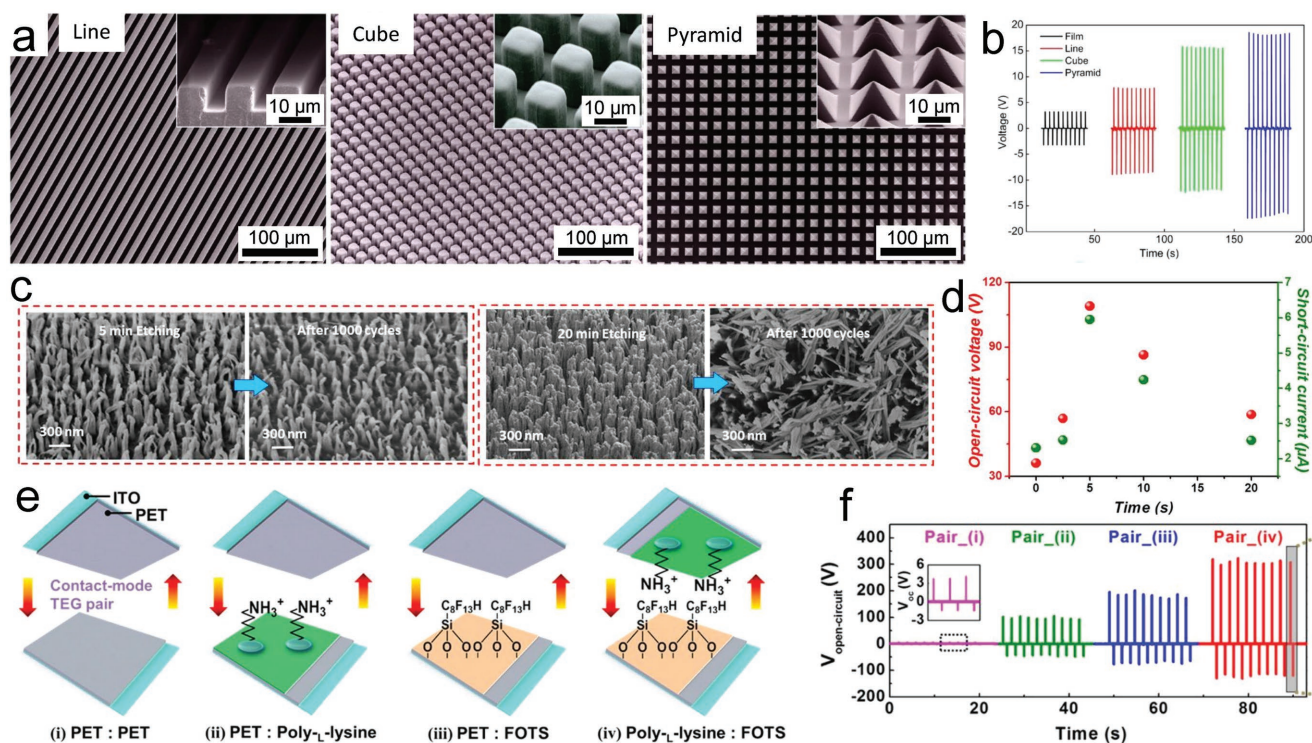


Figure 2. Surface modification of friction materials. a,b) SEM images of micron-pattern prepared by template method and the comparison of the output voltages of TENGs with four different surface types. Reproduced with permission.^[37] Copyright 2012, American Chemical Society. c,d) SEM images of nanowire arrays prepared by selective dry etching and the effect of time for etching polymer nanowires on output performance of TENG. Reproduced with permission.^[40] Copyright 2012, American Chemical Society. e,f) Comparison of the output voltage of TENGs with different surface functional groups. Reproduced with permission.^[41] Copyright 2015, American Chemical Society.

methods for preparing nanowire arrays on polymer surface are often used in boosting TENG output voltage. Zhu et al. used selective dry etching to create nanowire arrays on Kapton film, and it was concluded that the length of the nanowires significantly affected the output performance of TENG.^[40] Figure 2c shows the SEM images of the prepared nanowire arrays. For nanowires of the appropriate length with hundreds of nanometers, the elasticity can ensure the unchanged orientation and morphology after numerous contacts, as shown in Figure 2c. However, for excessively long nanowires (20 min etching), the strain generated at the root may exceed the elastic limit of the polymeric material when the materials contact, resulting in permanent deformation. The effect of time for etching polymer nanowires on V_{OC} and I_{SC} is shown in Figure 2d, which indicates that the electrical output rises significantly with etching time increasing from 0 to 5 min, while it drops dramatically with the excessive etching time.

On the other hand, the chemical modification by combining some appropriate functional groups on the surface can also effectively improve the output performance of TENG. Generally, when some functional groups that readily acquire electrons (such as $-CF_3$) are modified on the surface of the friction material, the friction surface will have a stronger affinity for the negative charges. In contrast, some functional groups that are prone to lose electrons (such as $-NH_2$) can generate a stronger affinity for the positive charge. As can be seen from Figure 2e, four different TENGs (i) PET:PET, (ii) PET:P-PET, (iii) PET:F-PET, and (iv) P-PET:F-PET) are prepared to verify whether the output

voltage is caused by different chemical bonds on the surface.^[41] To compare the output voltage of the four types of TENG, their V_{OC} were tested under the same conditions. Figure 2f shows the V_{OC} of four TENGs with a maximum output voltage (iv) P-PET:F-PET pair) more than 80 times higher compared to the voltage of the i) PET:PET pair. Yu et al. used sequential infiltration synthesis technique to infiltrate AlO_x molecules into polymer films and improved electrical properties of TENG.^[42] Since the AlO_x molecules have a strong tendency to repel electrons, the electron-acquisition ability of the AlO_x -doped polymer having strong electron affinity is remarkably lowered as compared with its original state, the corresponding output voltage is increased by a factor of ten. Hence, the combination of both physical and chemical modifications can finally achieve an optimized electrification performance for TENG.^[43]

2.3. Enhancement of TENG's Voltage Performance by Charge Injection Methods

The charge injection methods can directly increase the surface charge density to a saturation state. Therefore, the surface charge density of friction film after charge injection is several times larger than that of a common film. Researchers have explored several effective methods of charge injection, including high voltage corona discharge and ionized air injection. High voltage corona discharge has been used as a common means of increasing charge density.^[44] Figure 3a shows the sketch of

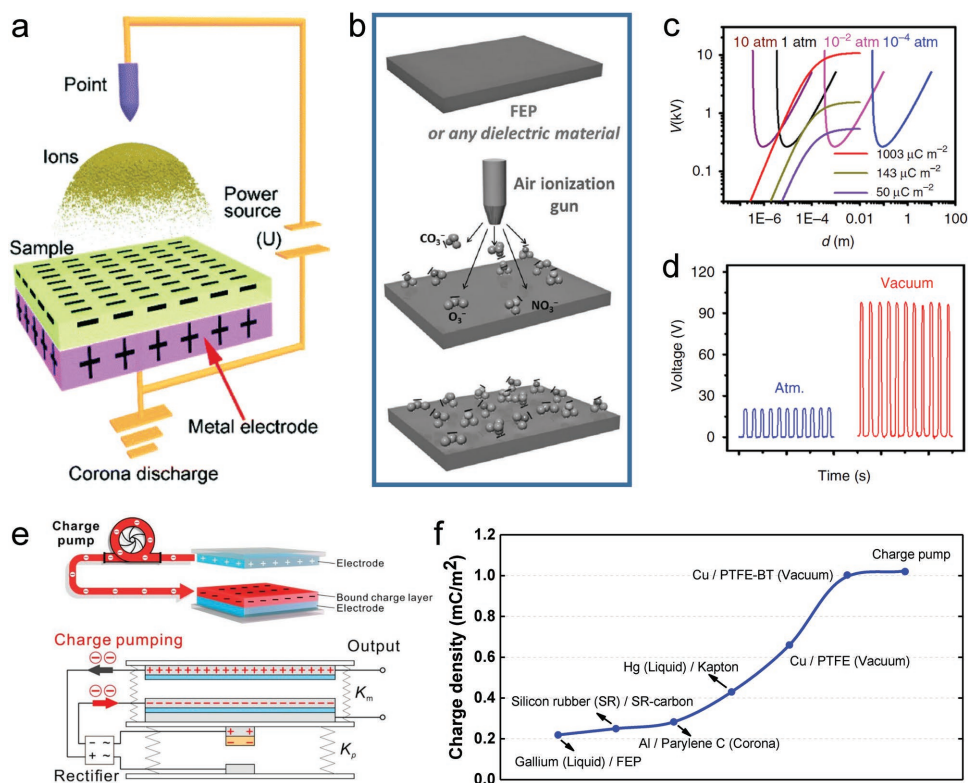


Figure 3. Charge injection methods and high voltage maintenance methods. a) The schematic of high voltage corona discharge for high voltage output of TENG. Reproduced with permission.^[45] Copyright 2017, Royal Society of Chemistry. b) Ionized-air injection for high performance of TENG. Reproduced with permission.^[47] Copyright 2014, Wiley-VCH. c) Theoretical breakdown voltage with different separation distance and theoretical output voltage of TENG with different charge densities. d) V_{OC} of the TENG in atmosphere as well as a high vacuum (with a vacuum of 10^{-6} Torr). c,d) Reproduced with permission.^[48] Copyright 2017, Nature Publishing Group. e) Schematic diagram of the charge pumping principle. Reproduced with permission.^[51] Copyright 2018, Elsevier. f) Comparison of high charge density achieved by different methods and materials.

the operating unit of the corona discharge, where a high voltage is formed between the needle tip and the dielectric layer.^[45] Shao et al. conducted a detailed research on the effects of high voltage corona discharge on TENG output performance.^[45] By using the corona discharge method, the V_{OC} is at least 55 times higher than the initial value. The peak voltage is related to the thickness of the dielectric layer, and the voltage of TENG also shows high cycle stability with a retention rate approaching 92.6% after 20 000 cycles. Hu et al. used both positive and negative corona discharging method to charge polypropylene film, the surface potential with negative corona decreased more slowly.^[46] Wang et al. utilized an air ionization gun to bring the negative ions (CO_3^- , NO_3^- , and O_3^-) onto the surface of FEP, as shown in Figure 3b.^[47] This method of introducing surface charges does not depend on the chemical properties of the surface. Through multiple ion implantation processes, the negative surface charges reach a high level, which has driven a fivefold increase in V_{OC} of TENG.

2.4. Vacuum Protection against Charge Leakage and Supplementary Charge Pump

As the surface charge density continues to increase, the increase in TENG output is limited by air breakdown. Hence, Wang et al. tested the output performance of TENG under

high vacuum.^[48] Figure 3c shows the air breakdown voltage with different air pressures and different charge densities of TENG. The Paschen's law in 1889 explains this phenomenon well.^[49] According to this phenomenon, the gap/output voltage of TENG must be smaller than the air breakdown voltage. Therefore, increasing the vacuum is also an effective way to increase the output of TENG. When the vacuum is 10^{-6} Torr, air breakdown is avoided in the operation of TENG, and the V_{OC} is increased by five times (Figure 3d). Similar to Bennet's charge doubler,^[50] by using the compensating circuit and structure design, Xu et al. proposed a facile and universal method to implement external charge compensation.^[51] As shown in Figure 3e, the designed TENG uses a floating layer to store and bind electrostatically induced charges, while another TENG as charge pump is designed to simultaneously pump charge into the floating layer.

Figure 3f shows the summarized values of high charge density achieved by several typical materials and methods. Zi et al. achieved a charge density of about 0.22 mC m^{-2} using triboelectrification between liquid Ga and FEP,^[52] while Tang et al. improved the value to 0.43 mC m^{-2} with liquid Hg and Kapton.^[13] Wang et al. fabricated silicon rubber mixed with carbon (SR-C) as a friction layer with the charge density of 0.25 mC m^{-2} .^[53] After high voltage corona discharge, the value of charge density achieves 0.28 mC m^{-2} for Al/Parylene C.^[45] Under high vacuum environment, the charge density can reach

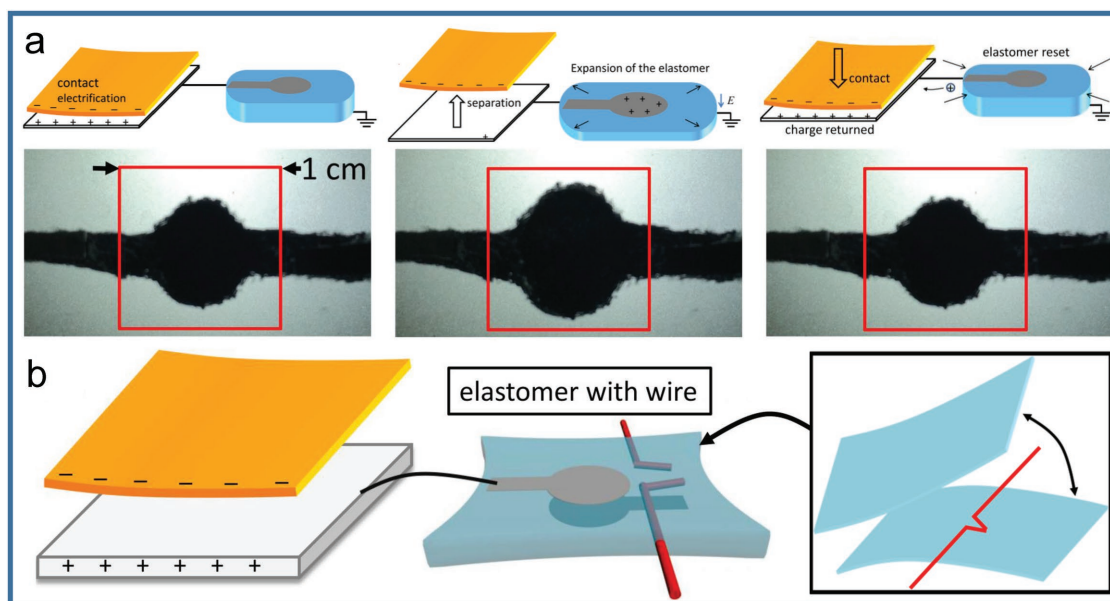


Figure 4. Self-powered artificial muscle and intelligent switch based on a TENG-based DEA system. a) Schematic of a TENG–DEA system with the strain performance and the photographs show the corresponding deformation of the DEA device. b) Working mechanism of a smart switch utilized the TENG–DEA system. Reproduced with permission.^[22] Copyright 2016, Wiley-VCH.

a high level of 0.66 mC m^{-2} for Cu/polytetrafluoroethylene (PTFE), and 1.003 mC m^{-2} with an extra ferroelectric layer.^[48] By changing the structure of TENG with a charge pump, a value of 1.02 mC m^{-2} is achieved.^[51]

3. Artificial Muscle Based on Dielectric Elastomer and TENG

Dielectric elastomer is a type of electro-active actuator material that exhibits excellent deformation ability under the stimulation of electric field; hence, the dielectric elastomer actuators (DEAs) have been applied for many applications, such as soft robotics and electronics, micropumps, and so on. The electric field in the thickness direction causes Maxwell stress, which leads to deformation of the elastomer.^[54] The working principle of DEA has long been well studied.^[55] With the characteristics of low elastic stiffness and large strain ability, the induced deformation of this DEA is significantly large and various functional mechanical actuators can be realized using this principle. However, the driving voltage for DEA is usually several thousand volts, which means that the actual application of DEA requires a high voltage source. As a choice, TENG has a characteristic of high output voltage with a small separation motion.^[8] By utilizing the high output voltage of TENG and large strain ability of DEA, a TENG–DEA system can be established, which is a good demonstration of TENG’s application in artificial muscles and soft actuators. Together with TENG’s energy harvesting capabilities, the drive system can achieve instantaneous interaction between human and the system, which allows it to be used as a self-powered drive component in micro electromechanical systems (MEMS) and human–machine interaction. In this section, several applications of TENG–DEA systems are presented, including artificial

muscles, intelligent switches, tunable smart optical modulator, and tunable optical gratings.

Figure 4a illustrates a simple demonstration of the TENG–DEA system using single-electrode TENG and a circular DEA.^[22] Two circular electrodes based on carbon grease are applied to the upper and lower sides of the elastomer film, while one electrode is connected to the TENG and the other electrode is grounded. To enhance the induced surface charge density, ICP treatment is used to prepare nanowire arrays covering the Kapton film for achieving a high surface area. After ICP treatment, the contact-separation movement of Kapton film and Al foil generates a high voltage between the electrode and the ground. Figure 4a shows the detailed working principle of the integrated system. Briefly, the contact between Kapton film and Al foil causes positive and negative charges at the contact interface. Then, the separation leads to a high electrostatic field on the dielectric elastomer, and the deformation of the DEA can be activated. The positive and negative charges are neutralized when this Kapton film and Al foil return to the original position, and then the deformation of DEA disappears. The excellent insulating properties and soft texture of the acrylic elastomer also allow the material to be used as a packaging material for soft electronic products. Figure 4b shows a demonstration of a smart switch by using the TENG–DEA system. The two wires are in contact with each other and sandwiched between the two elastomer films so that the connection and disconnection of the wires can be controlled by TENG. In this way, more functional performance can be achieved by printing complex circuits on the surface of the elastomeric film.

Based on the TENG–DEA system, Chen et al. proposed a smart optical modulator (SOM) by using silver nanowires as electrode materials.^[56] The electrode of the super-long silver nanowire can maintain good flexibility without sacrificing the

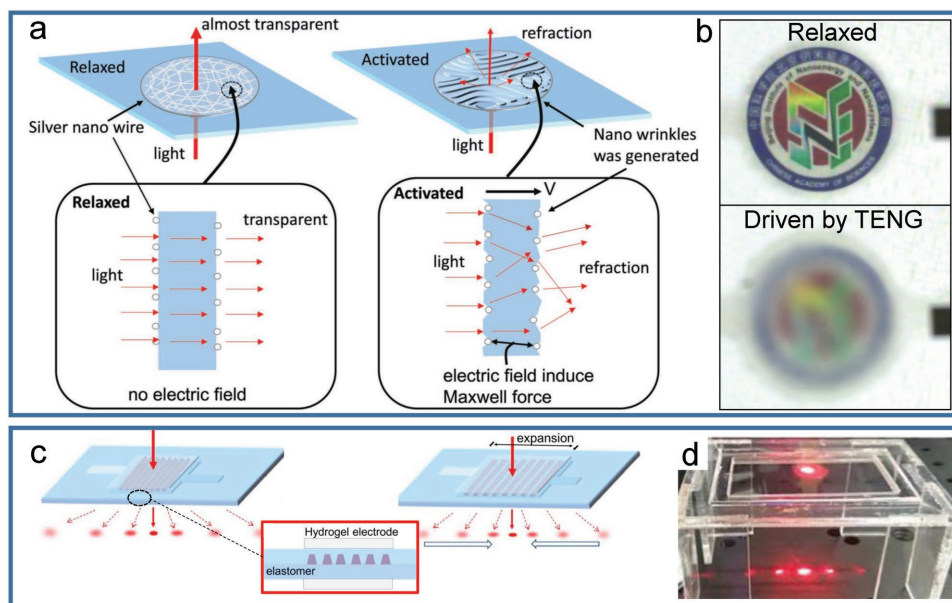


Figure 5. Intelligent optical modulator by coupling TENG and dielectric elastomer. a,b) The schematic of the working mechanism of the SOM driven by TENG and optical images through the SOM device. Reproduced with permission.^[56] Copyright 2017, Wiley-VCH. c,d) The sketch and optical image of TOGs with grating arrays driven by TENG. Reproduced with permission.^[57] Copyright 2017, Elsevier.

transparency and thus it can be applied for many tunable optical devices. **Figure 5a** shows the operating mechanism of the SOM device, which is similar to the ordinary DEA mentioned above. Before the activation, the SOM is transparent and stable. When a potential drop is applied to the elastomer, Coulomb attraction between the top and bottom nanowire electrodes leads to a localized microscopic deformation. These microscopic irregular deformations cause irregular refraction of light and result in a reduction in macroscopic transparency. The optical images modulated by SOM device are shown in **Figure 5b**, in which the transparent film becomes a matt film driven by TENG. Another application, tunable optical gratings (TOG), based on the similar TENG–DEA system has also been demonstrated, as shown in **Figure 5c**.^[57] When the actuation from the TENG causes the DEA element to expand, the grating period can be changed (**Figure 5c**). The corresponding optical images are shown in **Figure 5d**. The similar effect can also be applied for 2D optical grating and dot matrix grating, where the diffractive laser matrix can all be controlled by TENG. These designs and concepts of self-powered SOM and TOG systems can promote the application of TENG in optical communication, light capture, and other optical applications.

To achieve an effective control of the TENG–DEA system, a special operation method is also proposed, as shown in **Figure 6a**.^[56] By connecting two DEA units in series, a bias voltage is imposed in the whole system. Among the two DEA units, one is the target device and the other is the assistant device. Then, the output voltage of TENG can regulate the distribution of potential drop on two DEA units. As shown in **Figure 6a,b**, the contact of TENG decreases V_1 and increases V_2 , while the separation of TENG can increase V_1 and decrease V_2 . The applied voltage bias can help to overcome the threshold voltage value of DEA and the further increase of the applied voltage at this bias value can generate significant deformation for the target

DEA. As can be seen in **Figure 6b**, the SOM device is the target device and TENG can favorably control the deformation of this SOM. This method of increasing the external voltage bias is suitable for almost all DEA-related devices. Therefore, an elastomer-based electroluminescence device is also prepared based on this driving strategy (**Figure 6c**). The use of this driving strategy significantly enhances luminescence compared to TENG alone. **Figure 6d** shows the photograph of the device and the luminescence driving by this strategy. These two integrated devices demonstrate the great applicability of this operational strategy to DEA-related devices. Moreover, to better understand the working mechanism of the TENG–DEA system, a physical model has been constructed to simulate the effects of viscoelasticity and current leakage on TENG output performance.^[58] **Figure 6e,f** shows the theoretical model of the integrated system and the viscoelastic model of the elastomer, respectively. The comparison between the actual measurement and the simulation results is shown in **Figure 6g**, which confirms that this model is able to predict the response of DEA driven by TENG. This proposed physical model can help to better explore a variety of applications of TENG–DEA systems.

4. Micro-Actuators Based on Piezoelectric Ceramics and TENG

The piezoelectric materials can be deformed in an electric field, which is called the inverse piezoelectric effect. Generally, the deformation of the piezoelectric material is very small, while it has high precision and can be used for the precise operation of the microsystem. The most commonly used piezoelectric material is piezoelectric ceramics, which has been intensively applied for fabricating various electromechanical devices, such as ultrasonic motors, ceramic speaker, piezoelectric probe, and

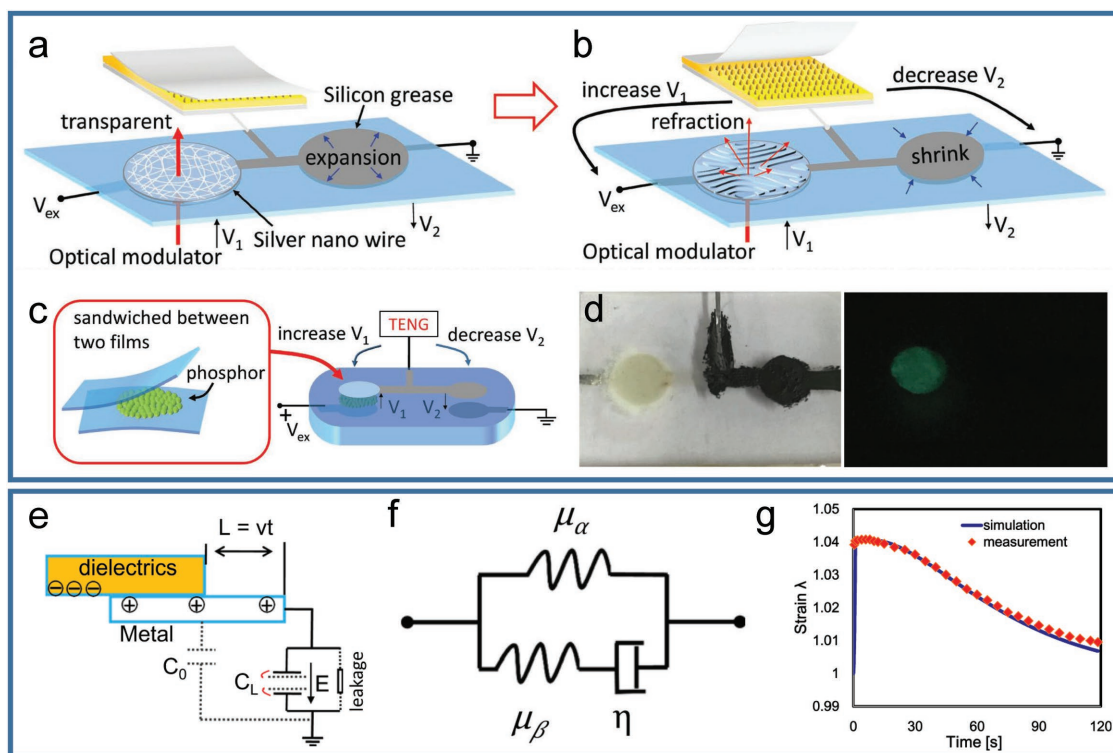


Figure 6. An effective method for operating the TENG–DEA system and theoretical analysis of the integrated system. a) A SOM and a DEA driven by a new method, where the output of TENG leads to activation strain of common DEA sample. b) The changes of transparency of SOM and the shrinkage of common DEA sample. c) A sketch of another application of the TENG–DEA system to illustrate the capability of special operation method. d) The optical image of the prepared sample and the generated luminescent behavior. a–d) Reproduced with permission.^[56] Copyright 2017, Wiley-VCH. e) Theoretical model for the TENG–DEA system. f) Theoretical model for viscoelasticity of the elastomer. g) The relaxation process of the actuated strain, where the dotted line is the experimental data and the solid line is the simulation results. e–g) Reproduced with permission.^[58] Copyright 2017, AIP Publishing.

so on. The driving voltage for piezoelectric ceramics is usually around dozens of volts, while the internal resistance of this material is high enough to maintain the tribo-induced charges. Hence, piezoelectric ceramics can be good materials to be coupled with TENG for realizing various self-powered electromechanical systems. By combining sliding TENG and piezoelectric ceramics, Zhang et al. proposed a piezoelectric micro-actuator for controlling the emission angle of a laser beam.^[23] Figure 7a shows the schematic of the designed three-layer sliding TENG, which consists of a PTFE film as free-standing triboelectric-layer and four Al foils as two pairs of orthogonal electrodes. To further increase the output voltage of TENG, the two surfaces of the PTFE film are treated by ICP to produce nanostructured morphology (Figure 7b). With this three-layer sliding TENG and piezoelectric bimorphs, optical modulation in 2D can be achieved by a designed active piezoelectric micro-actuator (Figure 7c). With the characteristics of precise deformation in an electric field, the piezoelectric micro-actuator can accurately control the direction of the laser. Another micro-actuator has also been developed with the three-layer sliding TENG and two variable infrared optical attenuators. Figure 7d shows the working principle of the electrostatic micro-actuator, and the dual channel optical modulation can be achieved by adjusting two infrared attenuators with TENG.

These TENG-based micro-actuators for optical modulation demonstrate the potential applications of piezoelectric materials in self-powered systems. In comparison with dielectric elastomers, the induced deformation of piezoelectric ceramics is much smaller. However, the deformation accuracy of dielectric elastomer can be influenced by its viscoelasticity, while piezoelectric ceramics can provide a better precision with a lower driving voltage. The dielectric elastomer with its soft and transparent texture can be possibly applied for artificial muscle or bionic devices, while piezoelectric materials are more suitable for the precise electromechanical system or ultrasonic devices. The combination of TENG and piezoelectric materials with the precise electrical deformation allows TENG to drive a series of micromachines. With the advantages of sustainable self-powered ability, these TENG-based micro-actuators will have broad application prospects in MEMS/NEMS.

5. Ferroelectric Materials Polarized by TENG for Memorization

Based on the integration of ferroelectric materials and TENGs, a new application has been developed for self-powered information memory system. The spontaneous polarization of the ferroelectric material responds well to the imposed electric field

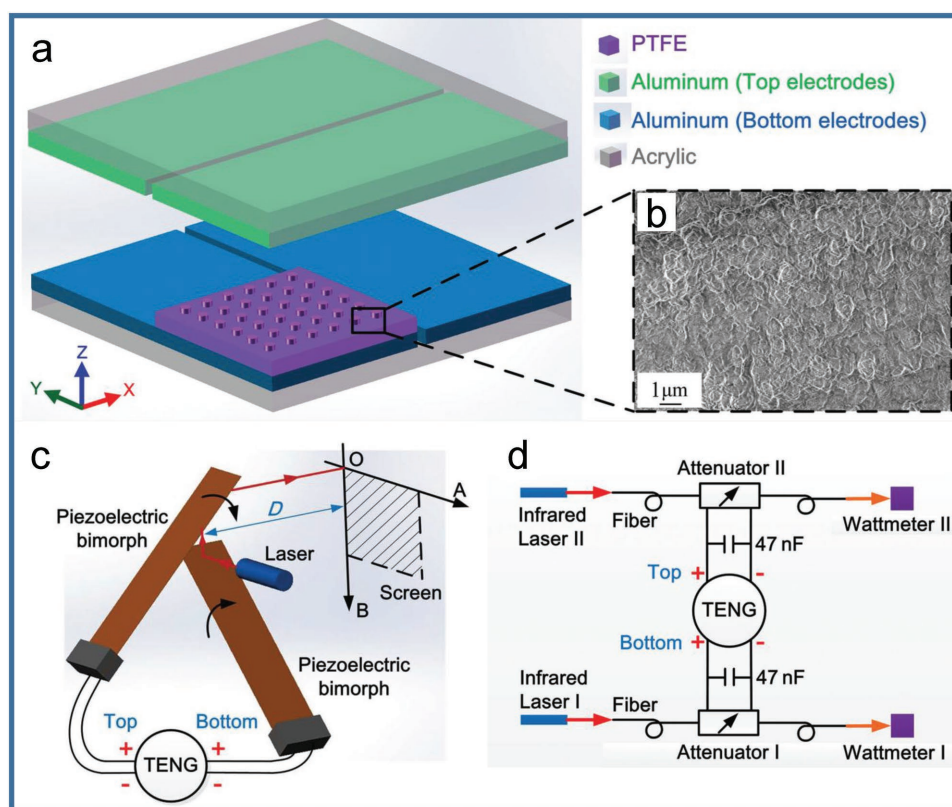


Figure 7. Optical modulated active microactuator based on planar sliding TENG. a) Schematic diagram of the designed three-layer sliding TENG. b) SEM image of the nanostructure of the PTFE membrane. c) A sketch of the structure of a 2D modulator driven by the three-layer sliding TENG. d) Schematic diagram of an active optical attenuator with two channels. Reproduced with permission.^[23] Copyright 2015, Wiley-VCH.

and is insensitive to current. This feature allows ferroelectric materials to be ideal for the output performance of TENG. In addition, the switching time of the dipole in the ferroelectric material is much smaller than the output period of the TENG. These factors determine that ferroelectric materials can be a good candidate to be coupled with TENG for realizing self-powered memory and storage devices.

With excellent repeatability of dipole switching, poly(vinylidene fluoride-trifluoroethylene) (P(VDF-TrFE)) has been widely studied in many devices. By combining TENG and P(VDF-TrFE) membrane, a unique self-powered memory system has been proposed for memorizing the motion in one and two dimensions.^[59] Figure 8a illustrates the self-powered memory system with sliding TENG and the corresponding working principle. In brief, when the electric field generated by the motion of TENG is applied on P(VDF-TrFE) film, the dipole moments in the film will be polarized. The electric field strength determines the magnitude of the polarization, so the memory system can record the displacement distance of the TENG. Then, the stored polarization information can be observed by a typical measurement with displacement-current, as shown in Figure 8b. In order to record the 2D motion trajectory, a self-powered storage system is prepared by a combination of a single-electrode TENG array and ferroelectric material (Figure 8c). Figure 8d,e shows the TENG array. The polarized ferroelectric materials can also be applied to enhance the output of TENG. Lee et al. use P(VDT-TrFE) and skin as

the contact materials in a single-electrode TENG,^[60] as shown in Figure 8f. After poling with the different electric field, the output voltage changes significantly and the skin potential can be controlled by the poling electric field applied on the P(VDT-TrFE) polymer.

The ferroelectric layer under the drive of TENG can also be used for recording a logical signal in electronic devices. Fang et al. designed a self-powered system for ferroelectric transistor memory by combining the high output of TENG and a field effect transistor (FET),^[24] as illustrated in Figure 9a. The rectified output voltage pulse of TENG is applied as a gate voltage to the ferroelectric transistor to control the channel. The binary states of FET can be read as a nonvolatile memory without alternately inverting the ferroelectric polarization. Figure 9b shows the ferroelectric property of the $0.65\text{Pb}(\text{Mg}_{1/3}\text{Nb}_{2/3})\text{O}_3-0.35\text{PbTiO}_3$ (PMN-PT) slice, which exhibits a p-type characteristics when the scan gate voltage is from -60 to 40 V. The typical $I_{\text{ds}}-V_{\text{ds}}$ characteristic of the pentacene ferroelectric transistor with different gate voltage is shown in Figure 9c, and the I_{ds} changes linearly with V_{ds} in the low-voltage region. To investigate the memory retention of such a self-powered system, a writing pulse generated by TENG is applied to FET. Figure 9d shows the $I_{\text{ds}}-V_{\text{ds}}$ curves, where the black curve indicates the OFF state and the red curve indicates the ON state. The bitable ON and OFF current states of this self-powered system demonstrate the excellent memory operation. The working mechanism of the storage system can utilize other various TENG so

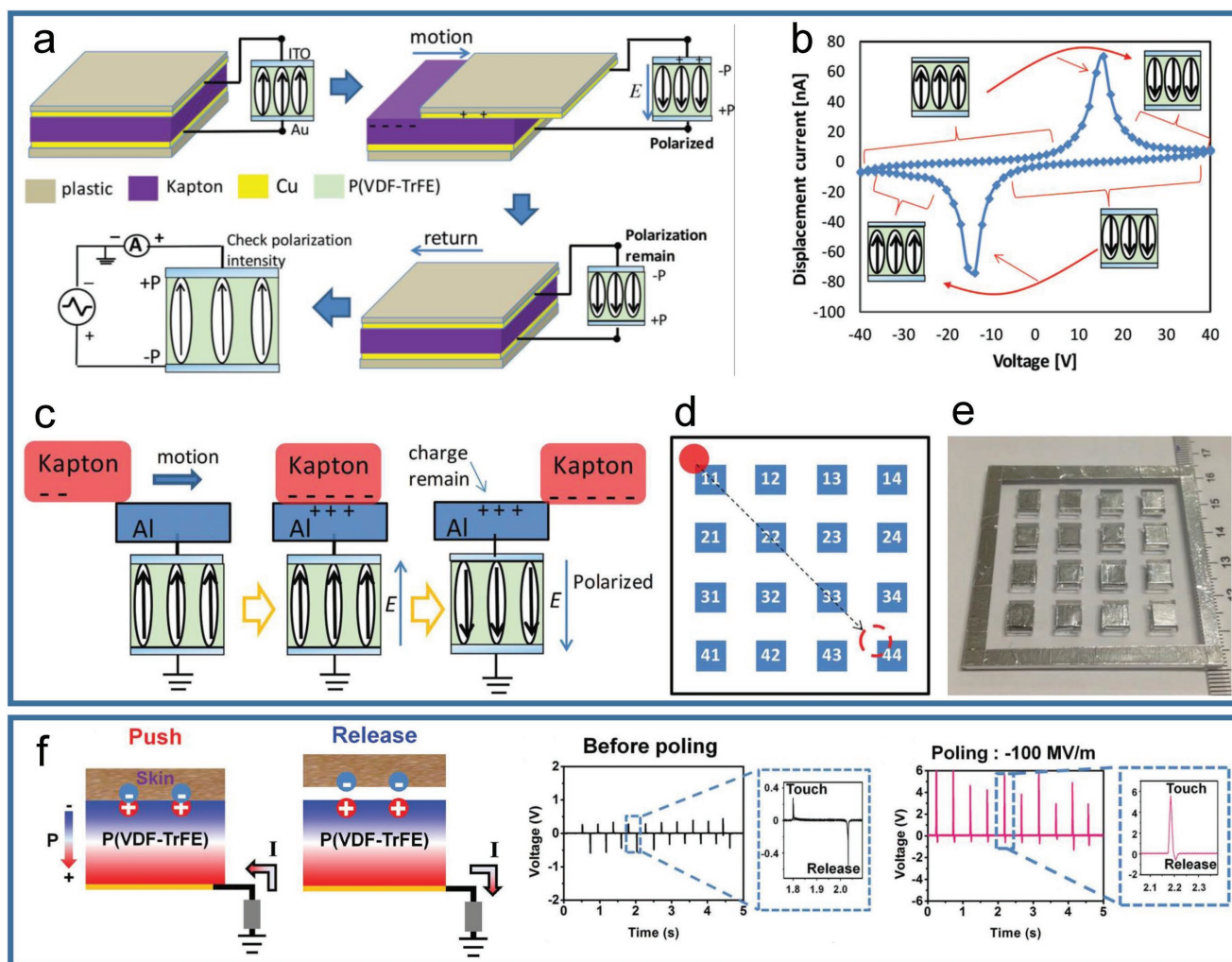


Figure 8. Self-powered trace memorized storage based on triboelectricity and ferroelectricity. a) Schematic diagram and working mechanism of the information storage device based on a TENG and a P(VDF-TrFE) film. b) The result of displacement current measurement of a device with a double circulation voltage (from -25 to 25 V). c) Schematic of the working mechanism of the memorized storage system by combining single-electrode TENG and P(VDF-TrFE). d) Sketch of a prepared TENG matrix for detecting and recording 2D motion trajectory. e) Photograph of the TENG matrix. a–e) Reproduced with permission.^[59] Copyright 2015, Wiley-VCH. f) Control of skin potential by triboelectricity with polarized P(VDF-TrFE) polymers. Reproduced with permission.^[60] Copyright 2015, Wiley-VCH.

that the ferroelectric materials ensure the application prospect of this memory technology. Hence, these systems can be applied as a self-powered storage disk or transistor for intelligent storage or smart electronic devices.

6. Electrostatic Manipulator Driven by TENG

The Coulomb force induced by the electrostatic field is the most straightforward electrically responsive effect and Coulomb force is the ideal driving force to manipulate macro/micro-objects. Accordingly, a series of applications based on this technique have been demonstrated in the field of smartphones, wearable products, micropump, and the microfluidic device.^[61] TENG can produce a strong electric field, and the leakage current through the electrostatic actuation device is very small. This phenomenon is good for maintaining tribo-charges. Moreover,

the finite amount of charge produced by TENG in one cycle can reduce the risk of electrical breakdown. Thus, the combination of TENG and electrostatic actuation system can achieve a motion-tunable electrostatic manipulator with self-powered ability. This TENG-based manipulator has the characteristics of fast response, high efficiency, and safety, the performance of which can be comparable with that of the commercial high voltage source. Hence, it can serve as an enabling technique for precisely manipulating tiny solid or liquid objects in MEMS systems, microfluidic channels, and many other application scenarios.

Wang et al. reported an electrostatic self-assembly method that facilitates the desired patterning of plastic pellets on a designed plate.^[62] Figure 10a shows the designed structure of the device, where a Teflon film with nanowire arrays on the surface (Figure 10b) is used as the electrification layer. By changing the shape of the grid electrode in the device structure, the

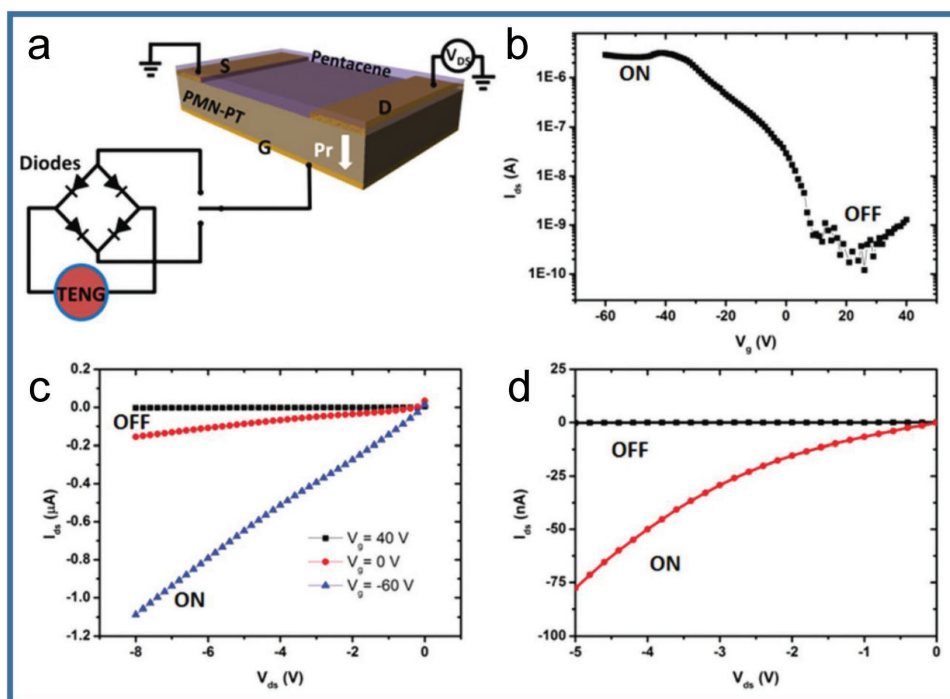


Figure 9. A self-powered nonvolatile ferroelectric transistor memory device integrated by TENG and a ferroelectric FET. a) Sketch of the self-powered transistor memory system. b) The transmission curve of the prepared transistor. c) Typical I_{ds} - V_{ds} characteristics of a pentacene ferroelectric transistor. d) I_{ds} with different V_{ds} supplied by TENG. By applying a positive gate voltage pulse with the TENG, the channel resistance remains large (OFF state). After applying a negative voltage pulse, the channel resistance is significantly reduced (ON state). Reproduced with permission.^[24] Copyright 2015, Royal Society of Chemistry.

desired self-assembly pattern can be obtained. A photograph of a sample with the assembled array is shown in Figure 10c, where the diameter of the nylon bead is 1.58 mm. The self-assembly principle is shown in Figure 10d,e in a cross-sectional view. In brief, after charging treatment with TENG, the surfaces of the nylon beads and electrification layer are positively and negatively charged, respectively. The positive charges induced by electrification layer flow from ground to the grid electrode, as shown in Figure 10d. Therefore, the electrostatic attraction between the beads and the window position is established (Figure 10e) and the beads are attracted to the window position. Zheng et al. also reported a similar TENG-based electrostatic actuator system for driving different motion of a metal pellet.^[63] As can be seen in Figure 10f, several disconnected ring electrodes are connected with segmented annular Al foils of TENG in a unique electrostatic actuator. The metal pellet is grounded with a carbon fiber, thus charges can be induced on the pellet. The electrostatic attraction between the electrode and the pellet is generated by the excitation of TENG. Accordingly, the circular motion of Kapton on the ring Al foils causes a rotating movement of the metal pellet. Another electrostatic actuator with pendulum structure is also designed (Figure 10g), where the motion of Kapton film in TENG can regulate the oscillation of the pellet.

The TENG can not only manipulate the movement of tiny solid objects but also control the motion of microfluidics. **Figure 11a** shows the structure and the operation process of a designed self-powered microfluidic manipulator, which can control the confluence of two droplets.^[63] The FEP film with

hydrophobic surface treatment acts as a dielectric layer in the self-powered system and water droplets can smoothly slide on the FEP surface. Two droplets are placed on two electrodes connected to TENG, one intermediate strip electrode is grounded. Then, the Coulomb force generated by TENG can drive the two droplets to move toward each other. Figure 11b shows that a phenolphthalein droplet and an alkaline droplet are merged together and turn red. Nie et al. further modified the operation of TENG for precisely manipulating microfluidics.^[25] The grating electrodes are coupled with freestanding TENG to achieve more accurate control of the droplet position. This system has superior operation reliability, which allows TENG to control the motion of a mini car (Figure 11c). The four microdroplets act as the wheels of the mini car, which is driven by the electrostatic force generated by TENG as a four-wheel drive. Moreover, the microdroplets can be driven by TENG on inclined or vertical planes, and it can even leap over one step, as shown in Figure 11d. To better understand the working principle of the microfluidic system driven by TENG, Nie et al. proposed a theoretical model for this combined self-powered system.^[64] Through the combination of finite element calculation and interpolation method, the motion behavior of the microdroplets driven by TENG is accurately simulated, the velocity of microdroplets can also be calculated.

Chen et al. also developed a droplet actuation system based on TENG, which used the energy of the triboelectrification between the water droplet and Teflon film.^[65] Figure 11e shows the devised structure and the working principle of this self-powered system, which consists of two chips: one fixed

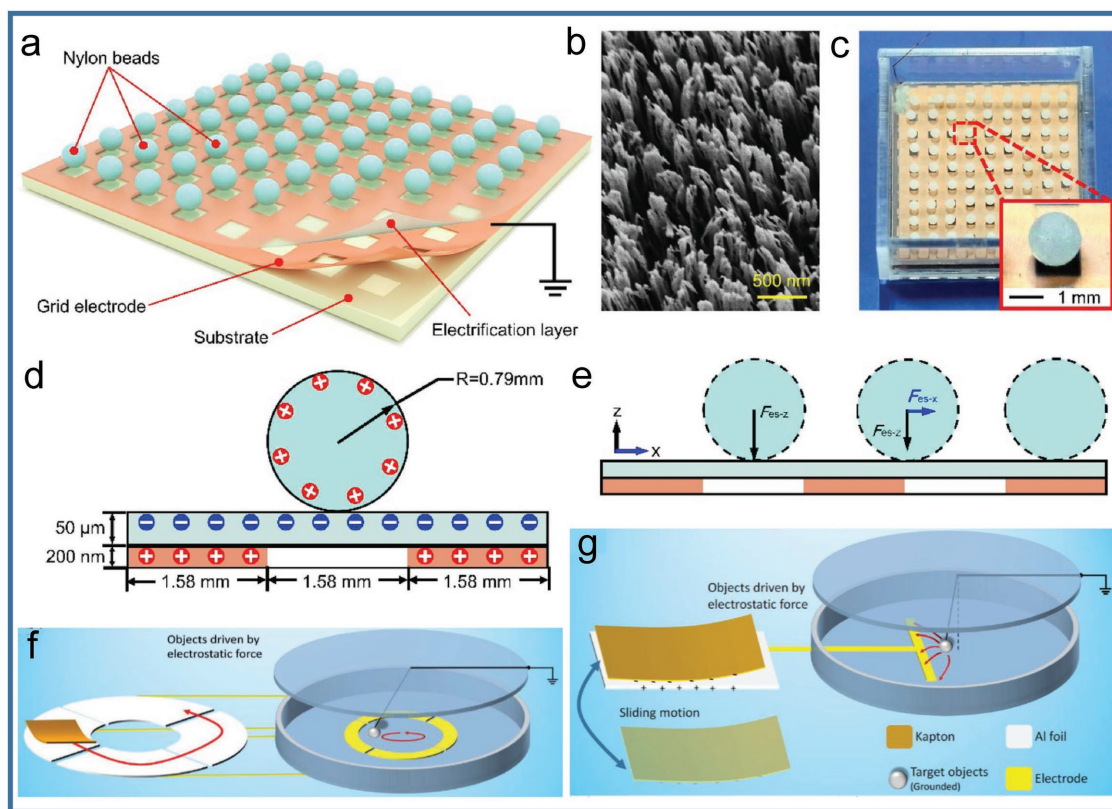


Figure 10. TENG as an electrostatic actuator for the manipulation of tiny objects. a) Structure of an electrostatic self-assembly device. b) SEM image of the Teflon surface morphology after plasma dry etching treatment. c) Photograph of the device with nylon balls. Inset: A close-up view of the nylon ball. d) Charge distribution of one nylon ball in one window. e) The electrostatic force of the ball at different locations. a–e) Reproduced with permission.^[62] Copyright 2018, American Chemical Society. f) The structure design of the self-powered electrostatic actuation system for leading rotated motion of a pellet. g) The electrostatic actuation system for swinging tiny object. f–g) Reproduced with permission.^[63] Copyright 2017, Wiley-VCH.

on a slanted frame as a sliding chip and the other fixed in the horizontal plane as an actuation chip. When droplets slide along the sliding chip, two electrodes on the sliding chip will induce different charges by electrification, which can generate a voltage signal in actuation chip. Accordingly, the contact angle of the droplets on the actuation chip changes, which generates a driving force to move the droplet. As can be seen in Figure 11e, by integrating four TENGs in an actuation system, the continuous motion of the droplet is achieved. The inset in Figure 11e is a photograph of the water droplet being driven to different positions. By changing the starting position of the droplets, the confluence of the two droplets is also achieved by this actuation system, as shown in Figure 11f. These TENG-based electrostatic manipulators can achieve accurate and effective manipulation of macro/microscale objects. Based on these integrated systems, a wide range of possible applications can be developed, including micromanipulators, microrobots, and target transport.

7. Electrostatic Adsorption and Air Cleaning Based on TENG

The Coulomb force generated by TENG can be used for accurately driving and manipulating tiny objects, and it can also be

applied for removing dust or pollutants in the open air, which leads to a self-powered electrostatic adsorption technology. Traditional electrostatic adsorption is an effective dust removal technology that usually requires a high voltage on the insulator filter. The high voltage and strong electric field generated by TENG can effectively absorb tiny particles. Meanwhile, TENG can convert the surrounding mechanical energy to maintain the high voltage of the filter. Thus, many TENG-based air purification devices have been proposed. With excellent advantages of simple structure, zero ozone release, high filtration efficiency, and low cost, these TENG-based air cleaning devices are applied for removing particulate matter from automobile exhaust fumes and indoor atmosphere. These TENG-based air cleaning devices have great commercial potential in the fields of haze treatment, air purification, volatile organic compounds (VOC) removal, and wearable devices for human health. Some well-established prototypes, such as “Circulating fresh air purifier” and “PaPa masks,” have already been marketed as commercial products by Nair TENG Company (www.nairteng.com).

Han et al. designed a self-powered filter for clearing away particulate matters (PMs) from motor vehicle emission by TENG.^[26] A vibration TENG (V-TENG) with two Al foils and many polymer pellets is prepared for the removal of PMs. Figure 12a shows the schematic of the V-TENG, and the high voltage is generated due to the collision motion between pellets

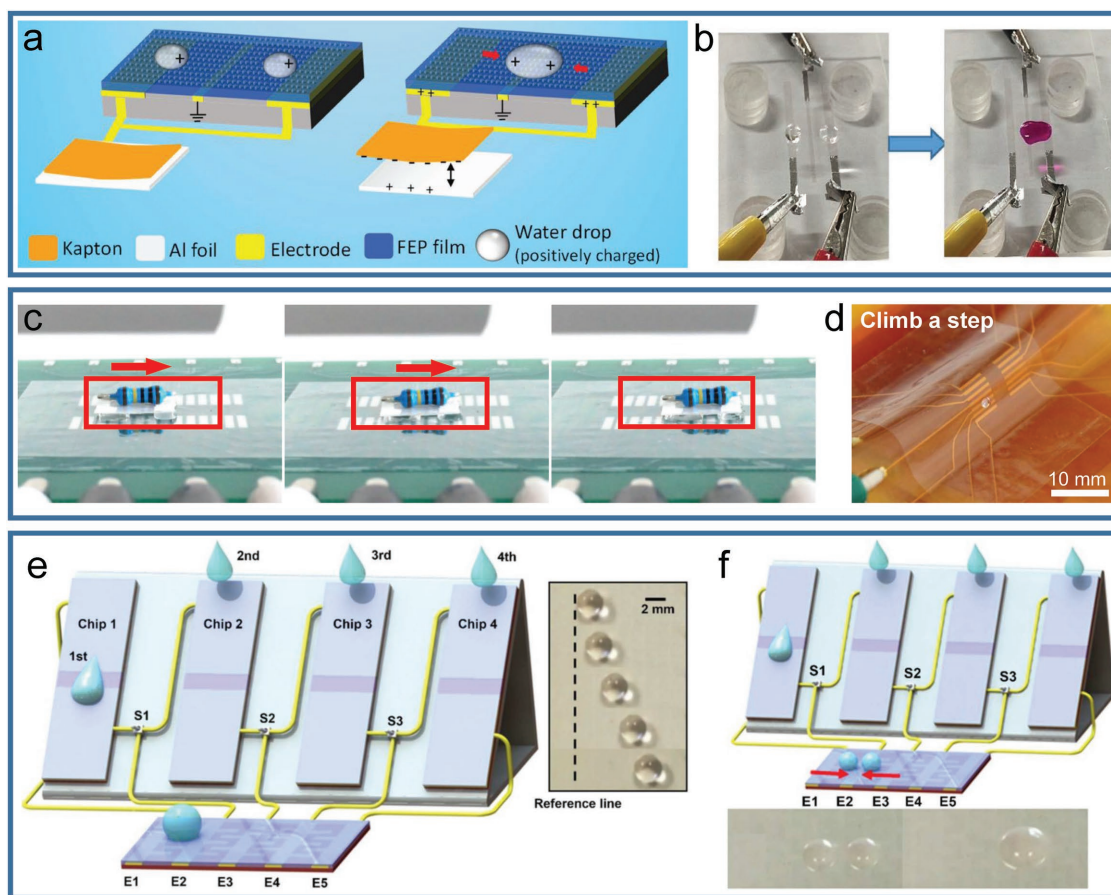


Figure 11. The manipulation of microfluidics by TENG in a microfluidic system. a) The design of the electrostatic actuation system for merging two droplets by TENG. b) The photographs of a phenolphthalein droplet and an alkaline droplet before and after the confluence. a,b) Reproduced with permission.^[63] Copyright 2017, Wiley-VCH. c) Photographs of a self-powered transport system with a mini car driving by TENG. d) A photograph of a droplet climbing a step based on the electrostatic actuation system. c,d) Reproduced with permission.^[25] Copyright 2018, American Chemical Society. e) Continuous droplet actuation on a chip connected with multiple TENG. f) Two droplets merging by a slip of a large droplet. e,f) Reproduced with permission.^[65] Copyright 2018, Royal Society of Chemistry.

and Al foils, which can be used to absorb the PMs. Figure 12b shows a photograph of the V-TENG and the inset is a photograph of PTFE pellets. Both ends of the V-TENG have exits for the air inlet and outlet. When the gas stream mixed with particulates passes through the V-TENG, the air stream can induce collision between PTFE pellets and Al foils. Then, the surface charges are generated on PTFE pellets due to triboelectrification, which can generate a strong electrostatic field to absorb the pollutant particulates. As can be seen in Figure 12a, the pollutant particulates in the gas stream are adsorbed by the pellets with strong electrostatic fields. As can be seen in Figure 12c, the V-TENG as a filter is fixed on a tailpipe of a car, where the vehicle emission directly enters the TENG through a long tube (inset in Figure 12c). The role of the long tube is also to reduce the temperature of the vehicle exhaust.

Afterward, Gu et al. proposed another strategy to enhance the efficiency of polyimide (PI) nanofiber air filter by using the high voltage performance of the TENG.^[66] The particulates filter is fabricated by electrospinning a PI nanofiber film on a stainless steel mesh. After being positively charged by the rotating TENG, an electric field forms around the stainless

steel mesh, resulting in the significant enhancement of PM removal efficiency. The high voltage of TENG can not only improve the adsorption efficiency of PMs but also enhance the degradation efficiency of harmful gas. Chen et al. proposed a TENG-based air filter to remove SO₂ and flying dust particulate.^[67] Moreover, Feng et al. developed a purifying filter based on the combination of TENG and photocatalysis techniques for simultaneously increasing the adsorption capacity of PMs and the photocatalytic degradation speed.^[68] Figure 13a shows the self-powered filter that removes particulates and VOC by combining TENG and photocatalysis material. In this filter, the photocatalyst is deposited on the polymer-coated steel mesh. When the filter is driven by TENG, the tribo-effect will induce a strong electric field between vertical and horizontal wires, which can enhance the adsorption rate of particulates (Figure 13b). On the other hand, the separation and the migration of photogenerated carriers in the photocatalyst can be enhanced by an electric field,^[69] thus the photocatalytic efficiency will be improved in the electric field of TENG. The working principle of the enhancement of photocatalytic degradation by TENG is shown in Figure 13c.

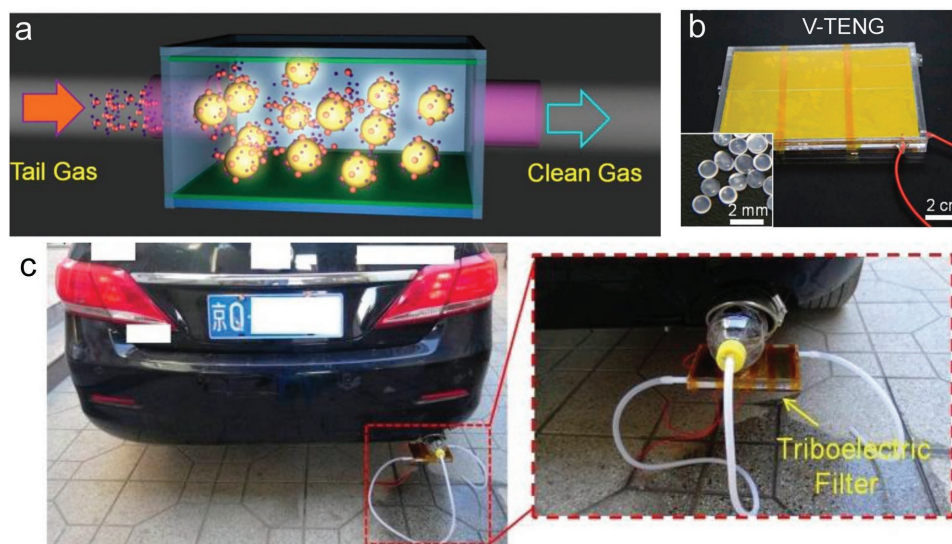


Figure 12. A self-powered air purifier for removing particulate matters from the exhaust of cars based on TENG. a) Sketch of the triboelectric effect for removing particulate matters in vibration TENG (V-TENG). b) Photograph of the V-TENG. Inset: A close-up view of the PTFE pellets. c) Photograph of the triboelectric purifier fixed on the tailpipe of a car. Inset: A partially enlarged image of the device. Reproduced with permission.^[26] Copyright 2015, American Chemical Society. Meanwhile, please note that the measurement of this device was done using a long tune so that the working temperature of the filter is almost at room temperature so that the filtering efficiency is high. However, once the working temperature is increased to 200 °C and above, the filtering efficiency reduces significantly.

TENG can also be easily designed with a variety of structures for portable and wearable air purification equipment. Liu et al. tactfully designed a self-powered electrostatic adsorption facemask based on a contact-separated TENG.^[70] Figure 13d shows the structure of this TENG-based facemask and the detailed working mechanism of the filtration. In this facemask, TENG acts as a breathing valve to absorb PMs from the air, and the TENG can continually provide electrostatic charges for improving removal efficiency. The SEM image of the polyvinylidene fluoride (PVDF) electrospun nanofiber film after absorption for 240 min continually is shown in Figure 13e, and the size distribution of the absorbed particulates is listed in the inset. Bai et al. also designed a washable facemask based on a simple TENG fabricated by PTFE and nylon fabrics.^[71] Moreover, Cheng et al. fabricated a facemask with two functions by using polyetherimide nanowire (fabricated by electrospun method), which can simultaneously remove particulates and monitor the human's respiratory rates.^[72]

8. Electronic Excitation, Ion Generation, and Microplasma Powered by TENG

Based on the electrostatic discharge effect of high electric field, several methods for ion or electron generation have been developed to promote the application of TENG for field emission and mass spectrometry. The amount of transferred charge of TENG can be precisely controlled by external parameters.^[9,73] By simply changing the sliding area or separation distance, TENG can produce different amount of transferred charge in the nC range, which is cumbersome for commercial power supplies. TENG can convert mechanical motion into a high-voltage output, which is convenient for obtaining a high electric field to

excite electrons. Meanwhile, the quantized charge generated by TENG can be used to precisely control the amount of electron emission, which is very beneficial for quantitative analysis and trace detection. These excellent performances open up a novel field for promoting economical, portable, and manageable light emitter, field emitter as well as mass spectrometry systems.

In 2015, Chen et al. used a single-electrode TENG to develop a self-powered field emission device (FED).^[74] The structure of the FED is shown in Figure 14a. This device consists of a carbon nanotube cathode and a phosphor/indium tin oxide (ITO) anode. The cathode and anode are separated by a thin glass spacer. As shown in Figure 14a, the amount of electrons emitted by the FED is controlled by the mechanical motion of the friction layer. The current density of the FED with different applied voltage is given in Figure 14b. Figure 14c shows a theoretical model to analyze the self-powered field emission device, which can help to better explore the application of the FED. Zi et al. utilized the high voltage of TENG to trigger the tribo-field emission and a more sophisticated emission system has been established.^[27] Figure 14d shows the schematic of the emitter, which has two electrodes made from ZnO nanowire arrays. In order to demonstrate the applicability of tribo-field emission, a commercial cathode-ray tube is powered by the TENG (Figure 14e). After only one sliding motion of the Teflon film in the TENG, the field emission is enabled in the cathode-ray tube (Figure 14f), and the illumination lasts for more than 100 min. With the improved controllability, portability, and stability, this tribo-induced field emitter can bring a new approach to traditional field emitting devices.

By utilizing TENG as an ion emission source, Li et al. developed a creative demonstration for self-powered mass spectrometric analysis.^[75] The total ionization charges in this TENG-based mass spectrometer can be quantitatively

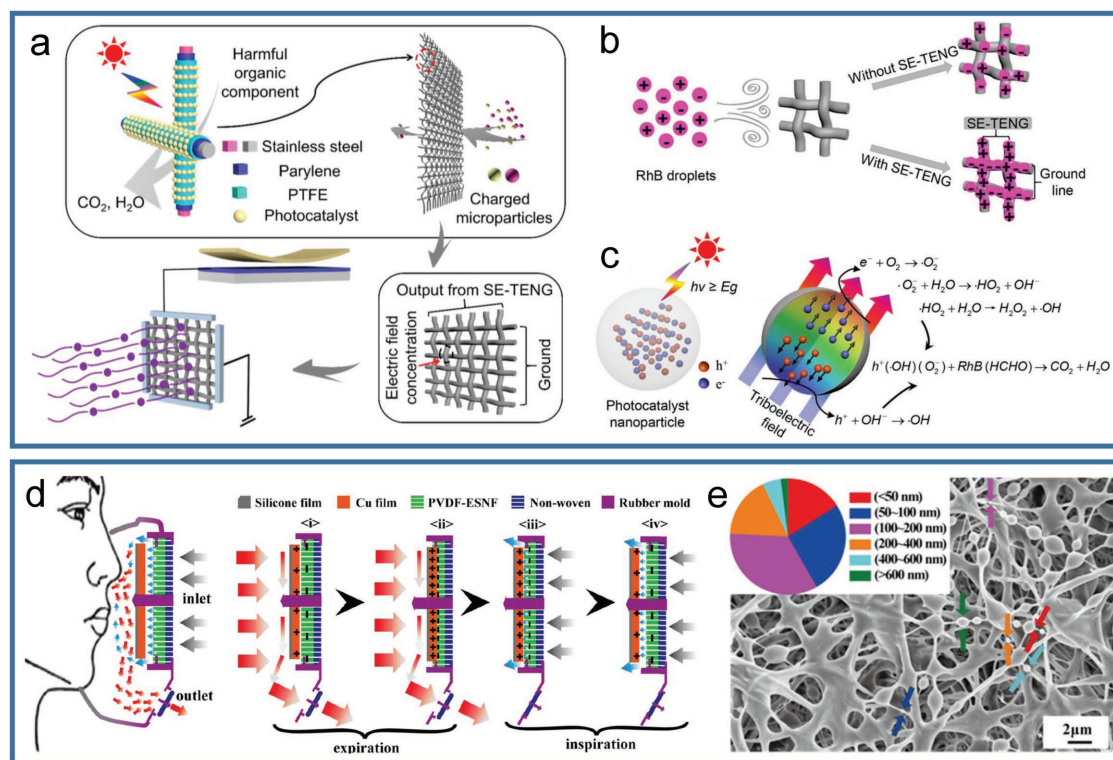


Figure 13. TENG-based air filter for efficient particulate matters removal. a) Schematic for self-powered absorption by electrostatic field and photocatalytic effect. b) Detailed schematic illustration of enhancement of electrostatic absorption by single electrode TENG. c) The enhancement of photocatalytic degradation of VOCs by TENG. a–c) Reproduced with permission.^[68] Copyright 2017, American Chemical Society. d) Structure and working mechanism of a self-powered electrostatic adsorption mask driven by respiration. e) SEM image of the PVDF nanofiber film after particulates filtration. Inset: The size distribution of the absorbed particulates. d,e) Reproduced with permission.^[70] Copyright 2018, American Chemical Society.

manipulated by adjusting the structure parameters of TENG. **Figure 15a,b** shows the coupling of TENGs and nanoelectrospray ionization emitter, where the single-polarity and alternating-polarity charge pluses can be generated by using TENG with both contact-separation mode (Figure 15a) and freestanding mode (Figure 15b). The limited charge from TENG can increase sample utilization, and the high voltage of TENG can guarantee the high sensitivity of nanoelectrospray ionization. Figure 15c shows the photographs of a nanoelectrospray ionization emitter driven by TENG. The generated charges can achieve plasma discharge ionization through a needle electrode. The equivalent circuit of this TENG-based mass spectrometry is shown in Figure 15d, where the TENG is symbolized by a capacitor (C_1) together with the components in the dashed rectangle on the left, the ion source is equivalent to a capacitor (C_2) and a resistor in the dashed rectangle on the right. The TENG mass spectrometer successfully analyzed a variety of compounds, including small organic molecules as well as large biomolecules. Bernier et al. also used this TENG-based mass spectrometry method to analyze genuine and falsified antimalarials.^[76] Figure 15e shows the schematic of a sliding freestanding TENG wooden-tip structure used in this test. When the top piece of the TENG device is manually moved from the grounded electrode toward the electrode connected to the toothpick, the positive ions are produced between toothpick and mass spectrometry inlet, as shown in Figure 15f. Conversely, negative ions are generated when the

top layer returns to the grounded side. By using TENG-powered toothpick electrospray, extracts of genuine and falsified antimalarials can be distinguished by mass spectrometry. Compared to other ion sources, triboelectric ion source produces similar information. TENG mass spectrometry method offers a simple, safe, and affordable way to generate ions, which can promote the development of portable and simple mass spectrometer for more convenient mass spectrometric analysis.

Plasma, as the fourth state of matters, is usually required to be generated by high temperature or through external electrical power sources. The equipment currently used to generate plasma usually needs to be sustained through external electrical power sources, which hinders the use of plasma in some scenarios where power is lacking. With a born character of high voltage, TENG can generate a high enough electric field in the operation and the discharge is very commonly observed, which demonstrates that TENG is very suitable for inducing continuous electrostatic discharge for plasma generation. Cheng et al. proposed an integrated system with a microplasma source and TENG to realize the atmospheric-pressure plasma production via mechanical stimuli.^[77] Microplasma is a plasma that is confined to a limited spatial extent. Since the discharge size is reduced to the millimeter level or even lower, the microplasma is generally capable of operating under atmospheric conditions. **Figure 16a** shows the schematic of the total device for atmospheric-pressure nonequilibrium plasma jets directly driven by a rotary TENG. The microplasma source in this system includes

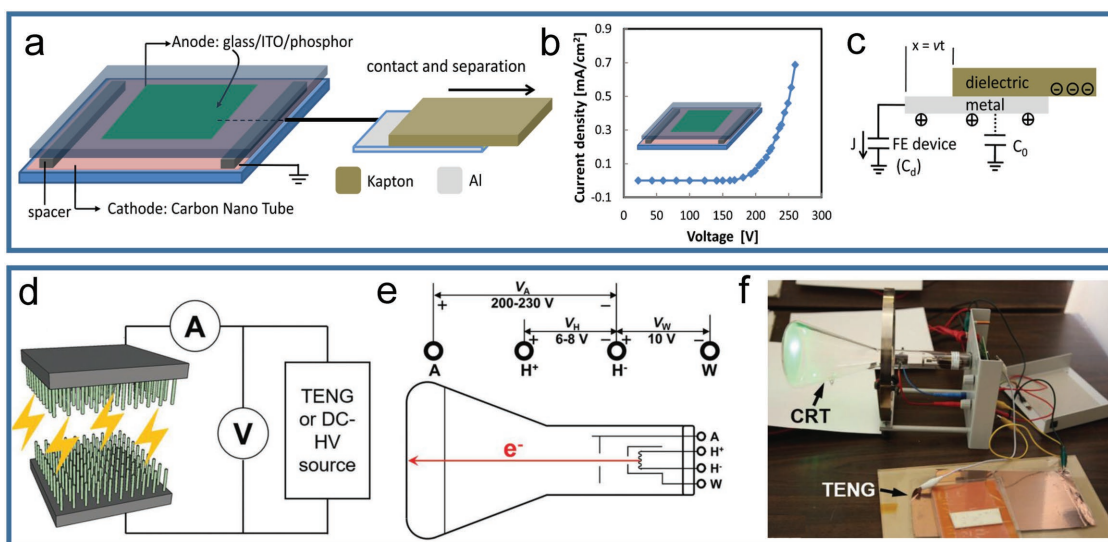


Figure 14. Field emission powered by TENG. a) Schematic diagram of a field emission device. b) J - V performance of the field emission device under the externally stable power supply. c) Theoretical model of the integrated self-powered system. a-c) Reproduced with permission.^[74] Copyright 2015, AIP Publishing. d) A schematic of an emitter, a power supply, and a measurement circuitry. e) The schematic diagram of the cathode ray tube with required power supply. f) A photograph of the successful display enabled by TENG. d-f) Reproduced with permission.^[27] Copyright 2018, Wiley-VCH.

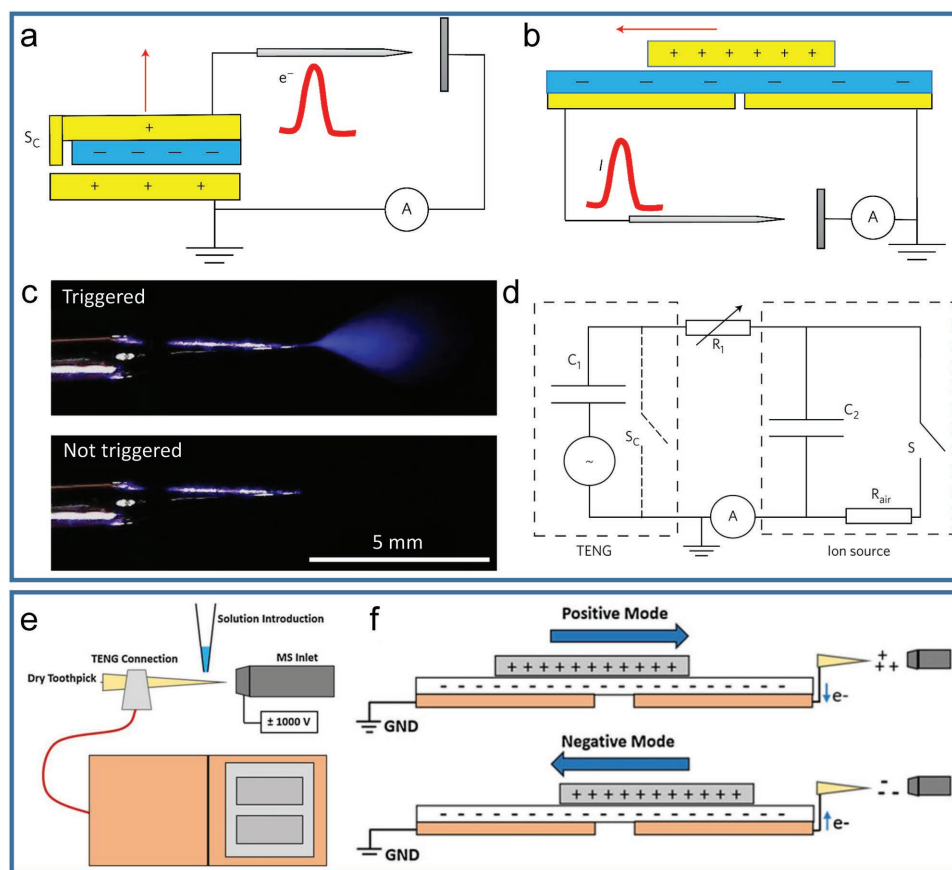


Figure 15. Mass spectrometry powered by TENG. a,b) Schemes of the ion generation mechanism with a) contact-separation and b) sliding freestanding mode TENGs. c) Darkfield images of the nanospray emitter showing the electro spray plume triggered by the TENG. d) An equivalent electronic circuit of this TENG-based mass spectrometry system. a-d) Reproduced with permission.^[75] Copyright 2017, Nature Publishing Group. e) Schematic of a sliding freestanding TENG wooden-tip setup used for mass spectrometry analysis of antimalarial tablets. f) The two TENG copper electrodes on the bottom layer are shown in light orange, while the sliding piece with lower charge density is shown in gray and the insulating middle layer is shown in white. e,f) Reproduced with permission.^[76] Copyright 2018, Wiley-VCH.

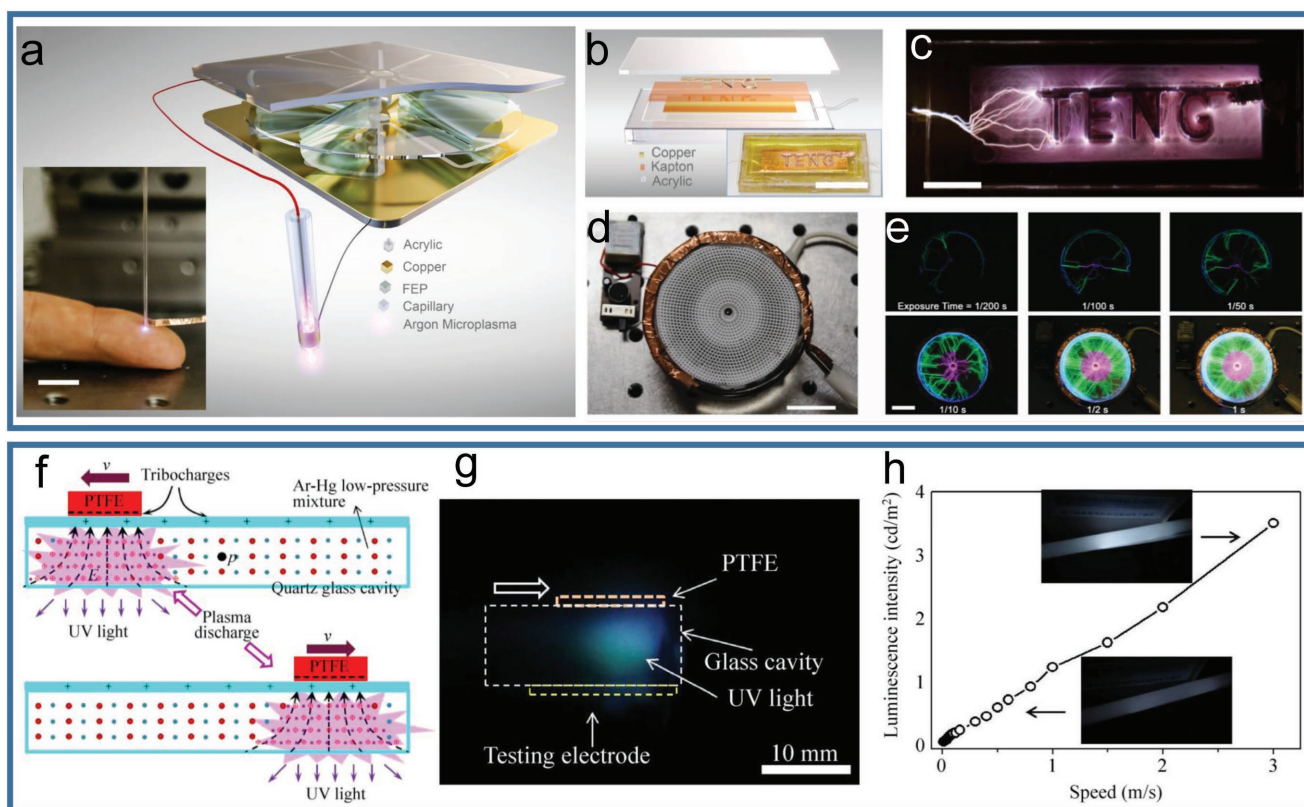


Figure 16. Triboelectric field-induced plasma discharge based on TENG. a) Schematic of an atmospheric-pressure nonequilibrium plasma jet directly driven by two serial freestanding rotary TENGs. Inset: Photograph of plasma jets on the skin of human finger (scale bar, 10 mm). b) Schematic of a patterned electrode dielectric barrier discharge plasma source. Inset: A photograph of the device (scale bar, 30 mm). c) A luminescence photograph of a patterned electrode directly driven by TENG (scale bar, 10 mm). d) A plasma disk driven by freestanding rotary TENGs. e) Photos with different exposure time. a–d) Reproduced with permission.^[77] Copyright 2018, Nature Publishing Group. f) Schematic of the working mechanism of a UV light-emitting device based on TENG and plasma discharge effect. g) A photograph of the UV emission in a glass cavity caused by friction between PTFE and glass. h) Luminous intensity with different sliding speeds of PTFE. Insets: Photographs of the luminescence. f–h) Reproduced with permission.^[78] Copyright 2014, Springer.

a glass capillary in which argon flows in the atmosphere, a metal wire electrode in the capillary, and an outer copper foil electrode. The triboelectric microplasma produced by our device can be visually observed, as shown in the inset of Figure 16a for the human finger. To demonstrate the plasma generated by TENG, a patterned electrode fabricated with copper and Kapton is placed in an acrylic box (Figure 16b). Under the direct drive of TENG, arc discharge and filament discharge occurred on the electrodes. This illuminating photograph of the device is shown in Figure 16c. Microplasma generated by TENG can replace traditional plasma in most application fields, such as materials treatment and discharge luminescence. One of the applications is luminescence, as shown in Figure 16d; a plasma disk is designed and powered by a rotating TENG. The illuminating photographs of the plasma disk with different exposure time are shown in Figure 16e. By changing material, structure or scale for the design and synthesis of different electrodes, such luminescence caused by triboelectric microplasma can be applied to a variety of different applications by mechanical stimulation alone.

Han et al. also utilized the TENG to bring plasma discharge for generating UV light emission.^[78] After rubbing between PTFE film and quartz glass tube, the surface of PTFE film is

negatively charged and the quartz cavity surface has positive charges. The high density of tribo-induced charges of the triboelectric layers leads to a strong electric field and then generates the plasma discharge in the Ar–Hg low-pressure gas (Figure 16f). When PTFE film slides on quartz glass, a violet plasma radiation is generated (Figure 16g). By exciting with the UV light generated by TENG, the visible light emission can be obtained. The light intensity increases as the sliding speed of the PTFE film increases (Figure 16h). The plasma excited by triboelectrification demonstrates that TENG can be used for generating diverse microplasma. Triboelectric plasma provides a novel complement to the use of plasma without the need for an additional power source. In the future, triboelectric plasma technology can be combined with different disciplines to produce a variety of plasma sources.

9. Summary and Perspectives

By using high voltage of TENG to directly drive or control some electrically responsive materials and devices, we can establish many self-powered composite systems with various functions. In this review, we have given the current progress of several

functional systems based on the combination of electrical devices and TENG. TENG is the ideal power source for directly driving devices and systems with large internal resistance, such as DEA, electrostatic manipulator, mass spectrometer, and other electrostatic devices. With a separation distance of few millimeters, the output voltage of TENG can easily reach several thousand volts. Moreover, TENG is able to control the voltage and transferred charge more conveniently by changing the contact area, sliding distance or separation distance compared with other high voltage power source. Substantial application of these self-powered systems has been demonstrated in the field of self-powered MEMS, intelligent storage systems, microfluidic systems, air cleaner, portable analytical instrument, and charge emission source. In the future, based on the cost-effectiveness and simple manufacturing process of TENG, the commercialization of TENG-based microfluidic chips, elastomeric smart optics, hand-held electrospinning machine, portable mass spectrometers, and many other self-powered systems may all become possible.

It is necessary to point out that high voltage source based on piezoelectric nanogenerator (PENG) or electret generator can also be realized. The output signal of PENG is decided by the applied force, while the output voltage from TENG is mainly dependent on the separation distance. Hence, TENG can utilize more kinds of motions, such as sliding motion or even suspension sliding. The electret generator is relying on electrostatic field and displacement current, which is quite similar to TENG. However, the electret generator must use the polarizable material, while the materials selection for TENG has a much wider range of options. More importantly, the previous study of electret generator is mainly focused on the MEMS chip and the increase of output signal. The concept of self-powered system is established by the researchers of nanogenerator, where the generated energy can be directly used to drive some devices or realize some promising functions, as we summarized in this review.

On the other hand, we conclude several future opportunities and challenges for TENG as the direct power source for electrically responsive materials and devices. The following research aspects need to be considered and more work should be focused on certain issues and constraints.

- 1) The continuous exploration of different materials and devices for coupling with TENG.

In order to achieve an effective and highly controllable system, the responsive materials and devices that can work with TENG may have several prerequisites. First, the target materials and devices are preferably a voltage-adjustable system for cooperating with TENG's characteristics of large output voltage and low output current. Second, the target materials and devices for coupling with TENG should have good insulating performance (capacitive device) to reduce leakage current, which can help to maintain the high voltage of TENG. Meanwhile, the target system should have low power consumption due to the limited charge transfer in a motion cycle of TENG. Finally, the target materials and devices should have some useful and unique functions, which can enrich the application scope of TENG-based self-powered systems.

- 2) The development of useful functions based on the characteristics of TENG.

The functions and effectiveness of the traditional electrically responsive materials and devices can be further developed by fully utilizing the merits of TENG. TENG has universal applicability and diversified structural design, which can be applied to a variety of application scenarios. In this way, many large operation systems can also be miniaturized based on TENG. The self-protection capability of TENG can facilitate its application for high voltage device, where the limited charges generated by TENG can reduce the risk of electrical breakdown. This feature is beyond the reach of traditional high-voltage power supplies. In addition, the TENG-based system can achieve instantaneous human-machine interaction, which can simplify the feedback/control circuits for the system.

- 3) The several challenges of the self-powered system based on TENG.

The output voltage of TENG is already high enough, while its output power still needs to be increased, in order to satisfy the system with larger energy consumption. More efforts can be concentrated on the preparation of advanced friction materials for a high power output. On the other hand, it is necessary to further improve the fine control of the output signal from TENG, in order to precisely regulate the operation of these systems in various environments. Two approaches may address this problem. One is to develop more environmentally stable tribo materials and thus the output of TENG can be more stable in different environments. Another method is to improve the insulating performance of the external systems, in order to suppress the leakage of the tribo-induced charges.

Supporting Information

Supporting Information is available from the Wiley Online Library or from the author.

Acknowledgements

The research was supported by the National Key R&D Project from Ministry of Science and Technology (2016YFA0202704), the "thousands talents" program for pioneer researcher and his innovation team, China, NSFC Key Program (Grant No. 21237003), National Natural Science Foundation of China (Grant Nos. 51775049, 51432005, 11674215, 5151101243, and 51561145021), and Young Top-Notch Talents Program of Beijing Excellent Talents Funding (2017000021223ZK03).

Conflict of Interest

The authors declare no conflict of interest.

Keywords

electrically responsive materials, electrostatic devices, self-powered functional systems, triboelectric nanogenerators

Received: September 7, 2018

Revised: November 3, 2018

Published online:

- [1] F.-R. Fan, Z.-Q. Tian, Z. Lin Wang, *Nano Energy* **2012**, *1*, 328.
- [2] Z. L. Wang, *Mater. Today* **2017**, *20*, 74.
- [3] a) T. Jiang, L. Zhang, X. Chen, C. Han, W. Tang, C. Zhang, L. Xu, Z. L. Wang, *ACS Nano* **2015**, *9*, 12562; b) L. Xu, Y. Pang, C. Zhang, T. Jiang, X. Chen, J. Luo, W. Tang, X. Cao, Z. L. Wang, *Nano Energy* **2017**, *31*, 351.
- [4] a) C. Zhang, W. Tang, C. Han, F. Fan, Z. L. Wang, *Adv. Mater.* **2014**, *26*, 3580; b) J. Chen, Y. Huang, N. Zhang, H. Zou, R. Liu, C. Tao, X. Fan, Z. L. Wang, *Nat. Energy* **2016**, *1*, 16138.
- [5] a) B. Chen, W. Tang, T. Jiang, L. Zhu, X. Chen, C. He, L. Xu, H. Guo, P. Lin, D. Li, J. Shao, Z. L. Wang, *Nano Energy* **2018**, *45*, 380; b) A. Yu, X. Chen, R. Wang, J. Liu, J. Luo, L. Chen, Y. Zhang, W. Wu, C. Liu, H. Yuan, M. Peng, W. Hu, J. Zhai, Z. L. Wang, *ACS Nano* **2016**, *10*, 3944.
- [6] Z. L. Wang, *Faraday Discuss.* **2014**, *176*, 447.
- [7] S. Niu, S. Wang, L. Lin, Y. Liu, Y. S. Zhou, Y. Hu, Z. L. Wang, *Energy Environ. Sci.* **2013**, *6*, 3576.
- [8] S. Niu, Y. Liu, S. Wang, L. Lin, Y. Zhou, Y. Hu, Z. L. Wang, *Adv. Mater.* **2013**, *25*, 6184.
- [9] S. Niu, Y. Liu, S. Wang, L. Lin, Y. S. Zhou, Y. Hu, Z. L. Wang, *Adv. Funct. Mater.* **2014**, *24*, 3332.
- [10] S. Niu, Y. Liu, X. Chen, S. Wang, Y. S. Zhou, L. Lin, Y. Xie, Z. L. Wang, *Nano Energy* **2015**, *12*, 760.
- [11] C. He, C. Han, G. Gu, T. Jiang, B. Chen, Z. Gao, Z. L. Wang, *Adv. Energy Mater.* **2017**, *7*, 1700644.
- [12] G. Zhu, Y. Zhou, P. Bai, X. Meng, Q. Jing, J. Chen, Z. L. Wang, *Adv. Mater.* **2014**, *26*, 3788.
- [13] W. Tang, T. Jiang, F. Fan, A. Yu, C. Zhang, X. Cao, Z. L. Wang, *Adv. Funct. Mater.* **2015**, *25*, 3718.
- [14] Y. Xie, S. Wang, S. Niu, L. Lin, Q. Jing, J. Yang, Z. Wu, Z. L. Wang, *Adv. Mater.* **2014**, *26*, 6599.
- [15] B. Chen, Y. Yang, Z. L. Wang, *Adv. Energy Mater.* **2018**, *8*, 1702649.
- [16] a) Z. L. Wang, *Nature* **2017**, *542*, 159; b) Z. L. Wang, T. Jiang, L. Xu, *Nano Energy* **2017**, *39*, 9; c) L. Xu, T. Jiang, P. Lin, J. Shao, C. He, W. Zhong, X. Chen, Z. L. Wang, *ACS Nano* **2018**, *12*, 1849.
- [17] a) W. Du, J. Nie, Z. Ren, T. Jiang, L. Xu, S. Dong, L. Zheng, X. Chen, H. Li, *Nano Energy* **2018**, *51*, 260; b) X. Chen, D. Taguchi, T. Manaka, M. Iwamoto, Z. L. Wang, *Sci. Rep.* **2015**, *5*, 13019; c) X. Chen, D. Taguchi, T. Manaka, M. Iwamoto, *Chem. Phys. Lett.* **2016**, *646*, 64.
- [18] Q. Tang, M.-H. Yeh, G. Liu, S. Li, J. Chen, Y. Bai, L. Feng, M. Lai, K.-C. Ho, H. Guo, C. Hu, *Nano Energy* **2018**, *47*, 74.
- [19] a) H. Guo, X. Pu, J. Chen, Y. Meng, M.-H. Yeh, G. Liu, Q. Tang, B. Chen, D. Liu, S. Qi, C. Wu, C. Hu, J. Wang, Z. L. Wang, *Sci. Rob.* **2018**, *3*, eaat2516; b) Z. Ren, J. Nie, J. Shao, Q. Lai, L. Wang, J. Chen, X. Chen, Z. L. Wang, *Adv. Funct. Mater.* **2018**, *28*, 1802989; c) X. Chen, Y. Wu, J. Shao, T. Jiang, A. Yu, L. Xu, Z. L. Wang, *Small* **2017**, *13*, 1702929; d) M. Ma, Q. Liao, G. Zhang, Z. Zhang, Q. Liang, Y. Zhang, *Adv. Funct. Mater.* **2015**, *25*, 6489.
- [20] Z. L. Wang, *ACS Nano* **2013**, *7*, 9533.
- [21] J. Chen, Z. L. Wang, *Joule* **2017**, *1*, 480.
- [22] X. Chen, T. Jiang, Y. Yao, L. Xu, Z. Zhao, Z. L. Wang, *Adv. Funct. Mater.* **2016**, *26*, 4906.
- [23] C. Zhang, W. Tang, Y. Pang, C. Han, Z. L. Wang, *Adv. Mater.* **2015**, *27*, 719.
- [24] H. Fang, Q. Li, W. He, J. Li, Q. Xue, C. Xu, L. Zhang, T. Ren, G. Dong, H. L. Chan, J. Dai, Q. Yan, *Nanoscale* **2015**, *7*, 17306.
- [25] J. Nie, Z. Ren, J. Shao, C. Deng, L. Xu, X. Chen, M. Li, Z. L. Wang, *ACS Nano* **2018**, *12*, 1491.
- [26] C. B. Han, T. Jiang, C. Zhang, X. Li, C. Zhang, X. Cao, Z. L. Wang, *ACS Nano* **2015**, *9*, 12552.
- [27] Y. Zi, C. Wu, W. Ding, X. Wang, Y. Dai, J. Cheng, J. Wang, Z. Wang, Z. L. Wang, *Adv. Funct. Mater.* **2018**, *28*, 1800610.
- [28] a) S. Niu, Y. Liu, Y. S. Zhou, S. Wang, L. Lin, Z. L. Wang, *IEEE Trans. Electron Devices* **2015**, *62*, 641; b) P. Jun, S. D. Kang, G. J. Snyder, *Sci. Adv.* **2017**, *3*, eaap8676.
- [29] a) T. Jiang, X. Chen, K. Yang, C. Han, W. Tang, Z. L. Wang, *Nano Res.* **2016**, *9*, 1057; b) J. Shao, T. Jiang, W. Tang, X. Chen, L. Xu, Z. L. Wang, *Nano Energy* **2018**, *51*, 688; c) J. Shao, T. Jiang, W. Tang, L. Xu, T. W. Kim, C. Wu, X. Chen, B. Chen, T. Xiao, Y. Bai, Z. L. Wang, *Nano Energy* **2018**, *48*, 292.
- [30] C. Xu, Y. Zi, A. C. Wang, H. Zou, Y. Dai, X. He, P. Wang, Y. C. Wang, P. Feng, D. Li, Z. L. Wang, *Adv. Mater.* **2018**, *30*, 1706790.
- [31] J. Henniker, *Nature* **1962**, *196*, 474.
- [32] D. K. Davies, *J. Phys. D: Appl. Phys.* **1969**, *2*, 1533.
- [33] B. Lee, The TriboElectric Series, <https://www.alphalabinc.com/triboelectric-series/> (accessed: August 2018).
- [34] J.-H. Lee, K. Y. Lee, M. K. Gupta, T. Y. Kim, D.-Y. Lee, J. Oh, C. Ryu, W. J. Yoo, C.-Y. Kang, S.-J. Yoon, J.-B. Yoo, S.-W. Kim, *Adv. Mater.* **2014**, *26*, 765.
- [35] G. Cheng, L. Zheng, Z.-H. Lin, J. Yang, Z. Du, Z. L. Wang, *Adv. Energy Mater.* **2015**, *5*, 1401452.
- [36] J. Luo, W. Tang, F. R. Fan, C. Liu, Y. Pang, G. Cao, Z. L. Wang, *ACS Nano* **2016**, *10*, 8078.
- [37] F. Fan, L. Lin, G. Zhu, W. Wu, R. Zhang, Z. L. Wang, *Nano Lett.* **2012**, *12*, 3109.
- [38] S. Lee, Y. Lee, D. Kim, Y. Yang, L. Lin, Z.-H. Lin, W. Hwang, Z. L. Wang, *Nano Energy* **2013**, *2*, 1113.
- [39] a) Y. Hu, J. Yang, Q. Jing, S. Niu, W. Wu, Z. L. Wang, *ACS Nano* **2013**, *7*, 10424; b) X. Wen, W. Yang, Q. Jing, Z. L. Wang, *ACS Nano* **2014**, *8*, 7405; c) H. Li, L. Su, S. Kuang, C. Pan, G. Zhu, Z. L. Wang, *Adv. Funct. Mater.* **2015**, *25*, 5691.
- [40] G. Zhu, C. Pan, W. Guo, C. Y. Chen, Y. Zhou, R. Yu, Z. L. Wang, *Nano Lett.* **2012**, *12*, 4960.
- [41] S. H. Shin, Y. H. Kwon, Y. H. Kim, J. Y. Jung, M. H. Lee, J. Nah, *ACS Nano* **2015**, *9*, 4621.
- [42] Y. Yu, Z. Li, Y. Wang, S. Gong, X. Wang, *Adv. Mater.* **2015**, *27*, 4938.
- [43] X.-S. Zhang, M.-D. Han, R.-X. Wang, B. Meng, F.-Y. Zhu, X.-M. Sun, W. Hu, W. Wang, Z.-H. Li, H.-X. Zhang, *Nano Energy* **2014**, *4*, 123.
- [44] T. Zhou, L. Zhang, F. Xue, W. Tang, C. Zhang, Z. L. Wang, *Nano Res.* **2016**, *9*, 1442.
- [45] J. Shao, W. Tang, T. Jiang, X. Chen, L. Xu, B. Chen, T. Zhou, C. Deng, Z. L. Wang, *Nanoscale* **2017**, *9*, 9668.
- [46] Q. Hu, B. Wang, Q. Zhong, J. Zhong, B. Hu, X. Zhang, J. Zhou, *Nano Energy* **2015**, *14*, 236.
- [47] S. Wang, Y. Xie, S. Niu, L. Lin, C. Liu, Y. S. Zhou, Z. L. Wang, *Adv. Mater.* **2014**, *26*, 6720.
- [48] J. Wang, C. Wu, Y. Dai, Z. Zhao, A. Wang, T. Zhang, Z. L. Wang, *Nat. Commun.* **2017**, *8*, 88.
- [49] F. Paschen, *Ann. Phys.* **1889**, *273*, 69.
- [50] A. Bennet, *Philos. Trans. R. Soc. London* **1787**, *77*, 288.
- [51] L. Xu, T. Bu, X. Yang, C. Zhang, Z. L. Wang, *Nano Energy* **2018**, *49*, 625.
- [52] Y. Zi, S. Niu, J. Wang, Z. Wen, W. Tang, Z. L. Wang, *Nat. Commun.* **2015**, *6*, 8376.
- [53] J. Wang, S. Li, F. Yi, Y. Zi, J. Lin, X. Wang, Y. Xu, Z. L. Wang, *Nat. Commun.* **2016**, *7*, 12744.
- [54] Z. Suo, *Acta Mech. Solida Sin.* **2010**, *23*, 549.
- [55] S. Bauer, S. Bauer-Gogonea, I. Graz, M. Kaltenbrunner, C. Keplinger, R. Schwojda, *Adv. Mater.* **2014**, *26*, 149.
- [56] X. Chen, X. Pu, T. Jiang, A. Yu, L. Xu, Z. L. Wang, *Adv. Funct. Mater.* **2017**, *27*, 1603788.
- [57] X. Chen, Y. Wu, A. Yu, L. Xu, L. Zheng, Y. Liu, H. Li, Z. L. Wang, *Nano Energy* **2017**, *38*, 91.
- [58] X. Chen, T. Jiang, Z. L. Wang, *Appl. Phys. Lett.* **2017**, *110*, 033505.
- [59] X. Chen, M. Iwamoto, Z. Shi, L. Zhang, Z. L. Wang, *Adv. Funct. Mater.* **2015**, *25*, 739.

- [60] J. H. Lee, R. Hinchet, T. Y. Kim, H. Ryu, W. Seung, H. J. Yoon, S. W. Kim, *Adv. Mater.* **2015**, *27*, 5553.
- [61] a) W. Kim, D. Choi, J.-Y. Kwon, D. Choi, *J. Mater. Chem. A* **2018**, *6*, 14069; b) X. Chen, D. Taguchi, T. Manaka, M. Iwamoto, *J. Appl. Phys.* **2012**, *111*, 113711; c) X. Chen, D. Taguchi, T. Manaka, M. Iwamoto, *Org. Electron.* **2013**, *14*, 320; d) X.-S. Zhang, M. Su, J. Brugger, B. Kim, *Nano Energy* **2017**, *33*, 393.
- [62] Y. Wang, X. Wei, S. Kuang, H. Y. Li, Y. Chen, F. Liang, L. Su, Z. L. Wang, G. Zhu, *ACS Nano* **2018**, *12*, 441.
- [63] L. Zheng, Y. L. Wu, X. Chen, A. F. Yu, L. Xu, Y. S. Liu, H. X. Li, Z. L. Wang, *Adv. Funct. Mater.* **2017**, *27*, 1606408.
- [64] J. Nie, T. Jiang, J. Shao, Z. Ren, Y. Bai, M. Iwamoto, X. Chen, Z. L. Wang, *Appl. Phys. Lett.* **2018**, *112*, 183701.
- [65] G. Chen, X. Liu, S. Li, M. Dong, D. Jiang, *Lab Chip* **2018**, *18*, 1026.
- [66] G. Gu, C. Han, C. Lu, C. He, T. Jiang, Z. Gao, C. Li, Z. L. Wang, *ACS Nano* **2017**, *11*, 6211.
- [67] S. Chen, C. Gao, W. Tang, H. Zhu, Y. Han, Q. Jiang, T. Li, X. Cao, Z. Wang, *Nano Energy* **2015**, *14*, 217.
- [68] Y. Feng, L. Ling, J. Nie, K. Han, X. Chen, Z. Bian, H. Li, Z. L. Wang, *ACS Nano* **2017**, *11*, 12411.
- [69] X. Chen, L. Liu, Y. Feng, L. Wang, Z. Bian, H. Li, Z. L. Wang, *Mater. Today* **2017**, *20*, 501.
- [70] G. Liu, J. Nie, C. Han, T. Jiang, Z. Yang, Y. Pang, L. Xu, T. Guo, T. Bu, C. Zhang, Z. L. Wang, *ACS Appl. Mater. Interfaces* **2018**, *10*, 7126.
- [71] Y. Bai, C. Han, C. He, G. Gu, J. Nie, J. Shao, T. Xiao, C. Deng, Z. L. Wang, *Adv. Funct. Mater.* **2018**, *28*, 1706680.
- [72] Y. Cheng, C. Wang, J. Zhong, S. Lin, Y. Xiao, Q. Zhong, H. Jiang, N. Wu, W. Li, S. Chen, B. Wang, Y. Zhang, J. Zhou, *Nano Energy* **2017**, *34*, 562.
- [73] a) T. Jiang, X. Chen, C. Han, W. Tang, Z. L. Wang, *Adv. Funct. Mater.* **2015**, *25*, 2928; b) S. Wang, Y. Xie, S. Niu, L. Lin, Z. L. Wang, *Adv. Mater.* **2014**, *26*, 2818.
- [74] X. Chen, T. Jiang, Z. Sun, W. Ou-Yang, *Appl. Phys. Lett.* **2015**, *107*, 114103.
- [75] A. Li, Y. Zi, H. Guo, Z. L. Wang, F. M. Fernandez, *Nat. Nanotechnol.* **2017**, *12*, 481.
- [76] M. C. Bernier, A. Li, L. Winalski, Y. Zi, Y. Li, C. Caillet, P. Newton, Z. L. Wang, F. M. Fernandez, *Rapid Commun. Mass Spectrom.* **2018**, *32*, 1585.
- [77] J. Cheng, W. Ding, Y. Zi, Y. Lu, L. Ji, F. Liu, C. Wu, Z. L. Wang, *Nat. Commun.* **2018**, *9*, 3733.
- [78] C. B. Han, C. Zhang, J. Tian, X. Li, L. Zhang, Z. Li, Z. L. Wang, *Nano Res.* **2015**, *8*, 219.